

The Large Hadron Electron Collider at CERN

An Introduction to the LHeC Project

Max Klein

University of Liverpool

Project

Deep Inelastic Scattering
Physics Programme

Two Accelerator Options
Detector Design

Outlook

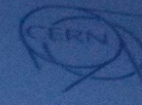


<http://cern.ch/lhec>

Seminar at University of Prague, 12.01.2012

DRAFT 1.0
Geneva, August 5, 2011
CERN report
ECEA report
NuPECC report
LHeC-Note-2011-001 GEN

M. Klein

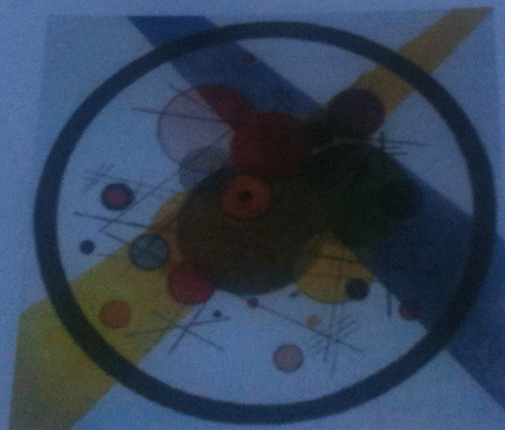


A Large Hadron Electron Collider at CERN

Report on the Physics and Design
Concepts for Machine and Detector

LHeC Study Group

THIS IS THE VERSION FOR REFEREEING, NOT FOR DISTRIBUTION



LHeC-Note-2011-003 GEN

To be submitted for publication

Draft LHeC Design Report
530 pages being refereed

Most of plots from CDR.

LHeC Study Group

J. Abelleira Fernandez^{10,15}, C. Adolphsen³⁹, S. Alekhin^{40,11}, A.N. Akai⁰¹, H. Aksakal³⁰, P. Allport¹⁷, J.L. Albacete³⁷, V. Andreev²⁵, R.B. Appleby²³, N. Armesto³⁸, G. Azuelos²⁶, M. Bai⁴⁷, D. Barber¹¹, J. Bartels¹², J. Behr¹¹, O. Behnke¹¹, S. Belyaev¹⁰, I. BenZvi⁴⁷, N. Bernard¹⁶, S. Bertolucci¹⁰, S. Bettoni¹⁰, S. Biswal³², J. Bluemlein¹¹, H. Boettcher¹¹, H. Braun⁴⁸, S. Brodsky³⁹, A. Bogacz²⁸, C. Bracco¹⁰, O. Bruening¹⁰, E. Bulyak⁰⁸, A. Bunyatian¹¹, H. Burkhardt¹⁰, I.T. Cakir⁵⁴, O. Cakir⁵³, R. Calaga⁴⁷, E. Ciapala¹⁰, R. Ciftci⁰¹, A.K. Ciftci⁰¹, B.A. Cole²⁹, J.C. Collins⁴⁶, J. Dainton¹⁷, A. De Roeck¹⁰, D. d'Enterria¹⁰, A. Dudarev¹⁰, A. Eide⁴³, E. Eroglu⁴⁵, K.J. Eskola¹⁴, L. Favart⁰⁶, M. Fitterer¹⁰, S. Forte²⁴, P. Gambino⁴², T. Gehrmann⁵⁰, C. Glasman²², R. Godbole²⁷, B. Goddard¹⁰, T. Greenshaw¹⁷, A. Guffanti⁰⁹, V. Guzey²⁸, C. Gwenlan³⁴, T. Han³⁶, Y. Hao⁴⁷, F. Haug¹⁰, W. Herr¹⁰, B. Holzer¹⁰, M. Ishitsuka⁴¹, M. Jacquet³³, B. Jeanneret¹⁰, J.M. Jimenez¹⁰, H. Jung¹¹, J.M. Jowett¹⁰, H. Karadeniz⁵⁴, D. Kayran⁴⁷, F. Kocac⁴⁵, A. Kilic⁴⁵, K. Kimura⁴¹, M. Klein¹⁷, U. Klein¹⁷, T. Kluge¹⁷, G. Kramer¹², M. Korostelev²³, A. Kosmicki¹⁰, P. Kostka¹¹, H. Kowalski¹¹, D. Kuchler¹⁰, M. Kuze⁴¹, T. Lappi¹⁴, P. Laycock¹⁷, E. Levichev³¹, S. Levonian¹¹, V.N. Litvinenko⁴⁷, A. Lombardi¹⁰, C. Marquet¹⁰, B. Mellado⁰⁷, K.H. Mess¹⁰, S. Moch¹¹, I.I. Morozov³¹, Y. Muttoni¹⁰, S. Myers¹⁰, S. Nandi²⁶, P.R. Newman⁰³, T. Omori⁴⁴, J. Osborne¹⁰, Y. Papaphilippou¹⁰, E. Paoloni³⁵, C. Pascaud³³, H. Paukkunen³⁸, E. Perez¹⁰, T. Pieloni¹⁵, E. Pilicer⁴⁵, A. Polini⁰⁴, V. Ptitsyn⁴⁷, Y. Pupkov³¹, V. Radescu¹³, S. Raychaudhuri²⁷, L. Rinolfi¹⁰, R. Rohini²⁷, J. Rojo²⁴, S. Russenschuck¹⁰, C.A. Salgado³⁸, K. Sampei⁴¹, E. Sauvan¹⁹, M. Sahin⁰¹, U. Schneekloth¹¹, A.N. Skrinsky³¹, T. Schoerner Sadenius¹¹, D. Schulte¹⁰, H. Spiesberger²¹, A.M. Stasto⁴⁶, M. Strikman⁴⁶, M. Sullivan³⁹, B. Surrow⁰⁵, S. Sultansoy⁰¹, Y.P. Sun³⁹, W. Smith²⁰, I. Tapan⁴⁵, P. Taels⁰², E. Tassi⁵², H. Ten. Kate¹⁰, J. Terron²², H. Thiesen¹⁰, L. Thompson²³, K. Tokushuku⁴⁴, R. Tomas. Garcia¹⁰, D. Tommasini¹⁰, D. Trbojevic⁴⁷, N. Tsoupas⁴⁷, J. Tuckmantel¹⁰, S. Turkoz⁵³, K. Tywoniuk¹⁸, G. Unel¹⁰, J. Urakawa⁴⁴, P. Van Mechelen⁰², A. Variola³⁷, R. Veness¹⁰, A. Vivoli¹⁰, P. Vobly³¹, R. Wallny⁵¹, G. Watt¹⁰, G. Weiglein¹², C. Weiss²⁸, U.A. Wiedemann¹⁰, U. Wienands³⁹, F. Willeke⁴⁷, V. Yakimenko⁴⁷, A.F. Zarnecki⁴⁹, F. Zimmermann¹⁰, F. Zomer³³

Project Milestones

2007: Invitation by SPC to ECFA and by (r)ECFA to work out a design concept

2008: First CERN-ECFA Workshop in Divonne (1.-3.9.08)

2009: 2nd CERN-ECFA-NuPECC Workshop at Divonne (1.-3.9.09)

2010: Report to CERN SPC (June)

3rd CERN-ECFA-NuPECC Workshop at Chavannes-de-Bogis (12.-13.11.10)

NuPECC puts LHeC to its Longe Range Plan for Nuclear Physics (12/10)

2011: Draft CDR (530 pages on Physics, Detector and Accelerator) (5.8.11)
being refereed and updated

2012: Publication of CDR – European Strategy
New workshop (tentatively in May 10-11, 2012)



Goal: TDR by 2014

Perspective: Operation by 2023 (synchronous with pp)

Organisation for CDR

Scientific Advisory Committee

Guido Altarelli (Roma)
Sergio Bertolucci (CERN)
Stan Brodsky (SLAC)
Allen Caldwell (MPI Muenchen) - Chair
Swapan Chattopadhyay (Cockcroft Institute)
John Dainton (Liverpool)
John Ellis (CERN)
Jos Engelen (NWO)
Joel Feltesse (Saclay)
Roland Garoby (CERN)
Rolf Heuer (CERN)
Roland Horisberger (PSI)
Young-Kee Kim (Fermilab)
Aharon Levy (Tel Aviv)
Lev Lipatov (St. Petersburg)
Karlheinz Meier (Heidelberg)
Richard Milner (MIT)
Joachim Mnich (DESY)
Steve Myers (CERN)
Guenther Rosner (Glasgow)
Alexander N. Skrinsky (INP Novosibirsk)
Anthony Thomas (JLab)
Steve Vigdor (Brookhaven)
Ferdinand Willeke (Brookhaven)
Frank Wilczek (MIT)



Steering Committee

Oliver Bruening(CERN)
John Dainton (Liverpool)
Albert De Roeck (CERN)
Stefano Forte (Milano)
Max Klein (Liverpool) - Chair
Paul Laycock (Liverpool)
Paul Newman (Birmingham)
Emmanuelle Perez (CERN)
Wesley Smith (Wisconsin)
Bernd Surrow (MIT)
Katsuo Tokushuku (KEK)
Urs Wiedemann (CERN)
Frank Zimmermann (CERN)

Working Group Convenors

Accelerator Design

Oliver Bruening (CERN)
John Dainton (Liverpool)

Interaction Region

Bernhard Holzer(CERN)
Uwe Schneekloth (DESY)
Pierre van Mechelen (Antwerpen)

Detector Design

Peter Kostka (DESY)
Alessandro Polini (Bologna)
Rainer Wallny (Zurich)

New Physics at Large Scales

Georges Azuelos (Montreal)
Emmanuelle Perez (CERN)
Georg Weiglein (Hamburg)

Precision QCD and Electroweak

Olaf Behnke (DESY)
Paolo Gambino (Torino)
Thomas Gehrmann (Zurich)
Claire Gwenlan (Oxford)

Physics at High Parton Densities

Néstor Armesto (Santiago de Compostela)
Brian A. Cole (Columbia)
Paul R. Newman (Birmingham)
Anna M. Stasto (PennState)

Review ongoing:

CERN Referees

Ring Ring Design

Kurt Huebner (CERN)
Alexander N. Skrinsky (INP Novosibirsk)
Ferdinand Willeke (BNL)

Linac Ring Design

Reinhard Brinkmann (DESY)
Andy Wolski (Cockcroft)

Kaoru Yokoya (KEK)

Energy Recovery
Georg Hoffstaetter (Cornell)
Ilan Ben Zvi (BNL)

Magnets

Neil Marks (Cockcroft)
Martin Wilson (CERN)

Interaction Region

Daniel Pitzl (DESY)
Mike Sullivan (SLAC)

Detector Design

Philippe Bloch (CERN)
Roland Horisberger (PSI)

Installation and Infrastructure

Sylvain Weisz (CERN)

New Physics at Large Scales

Cristinel Diaconu (IN2P3 Marseille)
Gian Giudice (CERN)

Michelangelo Mangano (CERN)

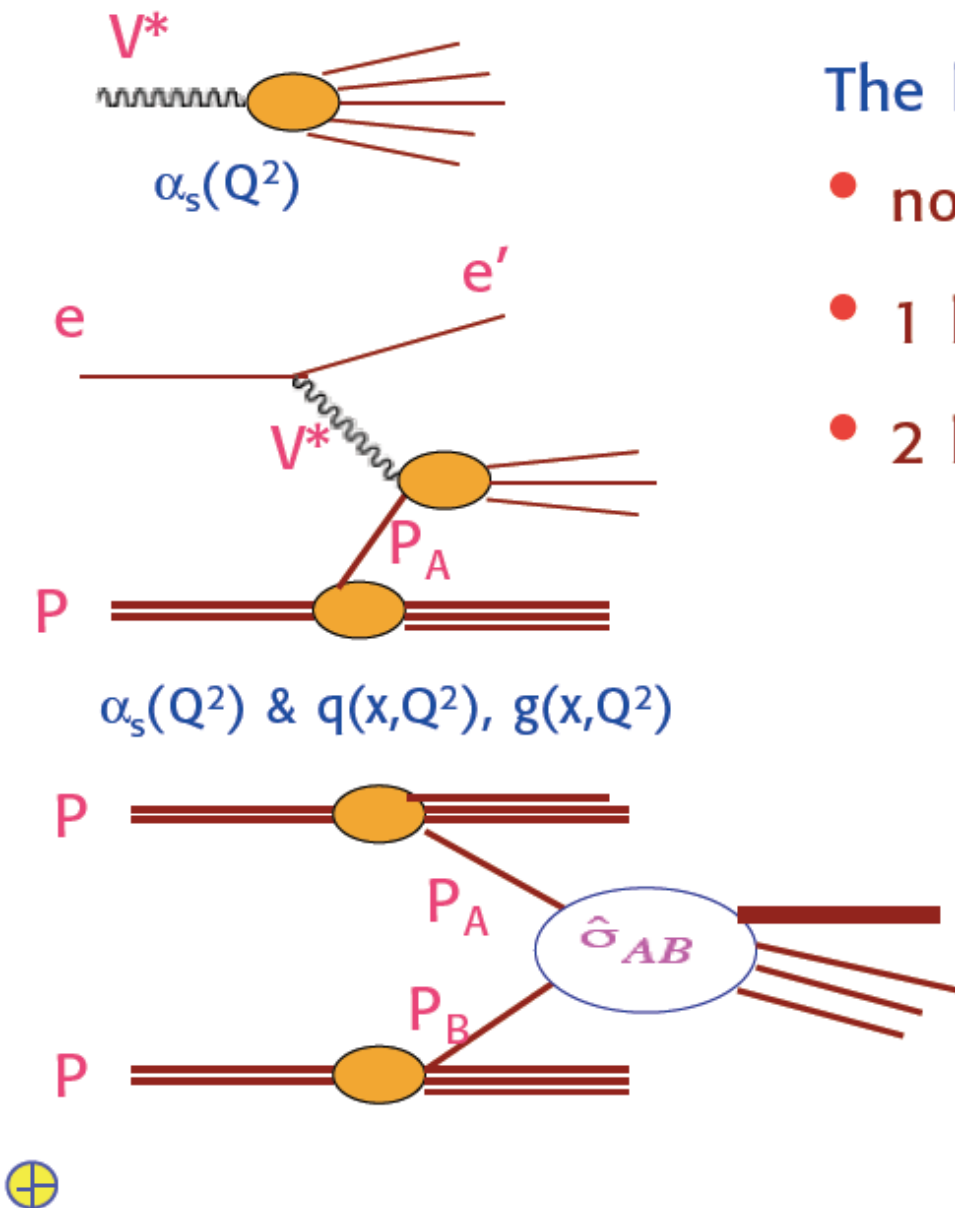
Precision QCD and Electroweak

Guido Altarelli (Roma)
Vladimir Chekelian (MPI Munich)
Alan Martin (Durham)

Physics at High Parton Densities

Alfred Mueller (Columbia)
Raju Venugopalan (BNL)
Michele Arneodo (INFN Torino)

I. Deep Inelastic Scattering, HERA,LHC and Physics at the LHeC

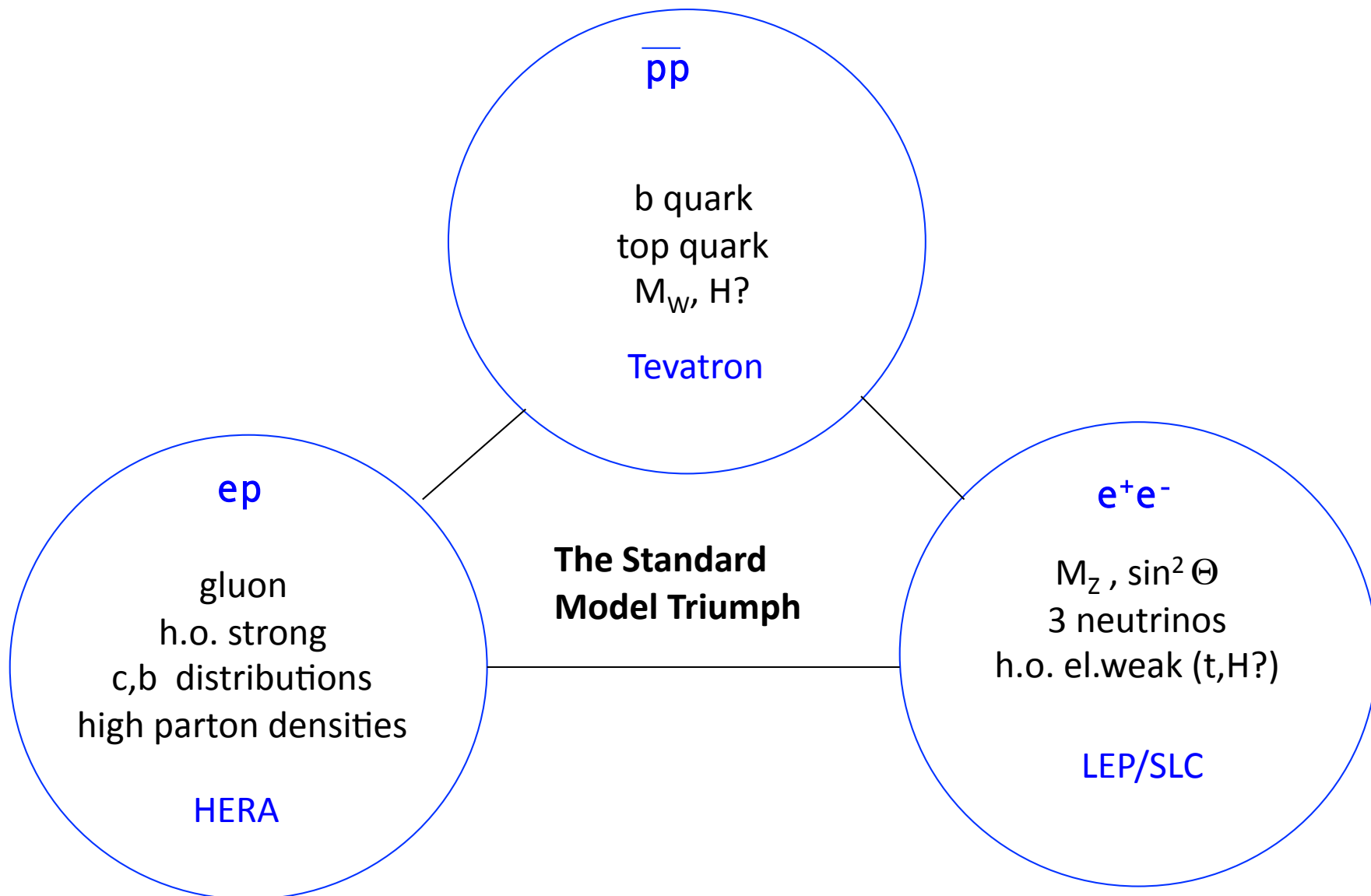


The basic experimental set ups:

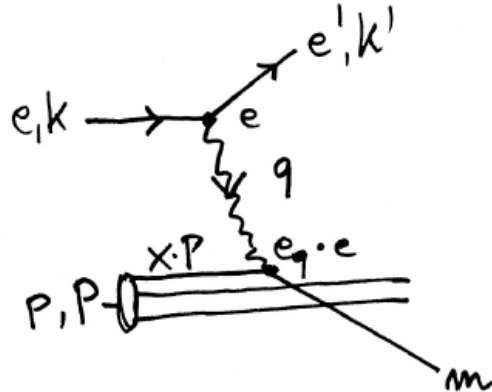
- no initial hadronLEP, ILC, CLIC
- 1 hadronHERA, LHeC
- 2 hadronsSppS, Tevatron, LHC

Progress in particle physics
needs their continuous
interplay to take full
advantage of their
complementarity

The Fermi Scale [1985-2010]



Deep Inelastic Scattering



"fixed target":

$$P = (M_p, 0, 0, 0)$$

$$2Pq = 2M_p(E - E')$$

$$= 2M_p E \cdot \frac{v}{E} \equiv s \cdot y$$

$$Q^2 = sxy \leq s$$

$$s = 2M_p E$$

$$s = 4E_e E_p$$

$$x = \frac{Q^2}{sy}$$

- ep collider

$$q = (k - k')$$

$$(xP + q)^2 = m^2, P^2 = M_p^2$$

$$Q^2 = -q^2 > 0$$

$$\text{if } Q^2 \gg x^2 M_p^2, m^2 :$$

$$q^2 + 2xPq = 0 :$$

$$x = \frac{Q^2}{2Pq}$$

$$\sigma(ep \rightarrow eX) = \frac{d^2\sigma}{dx dQ^2} \approx \frac{2\pi\alpha^2}{Q^4} (1 + (1 - y)^2) \cdot F_2$$

$$F_2(x, Q^2) = x \sum_q e_q^2 (q + \bar{q}), q = u, d, s, c, b, t$$

$$q = q(x, Q^2)$$

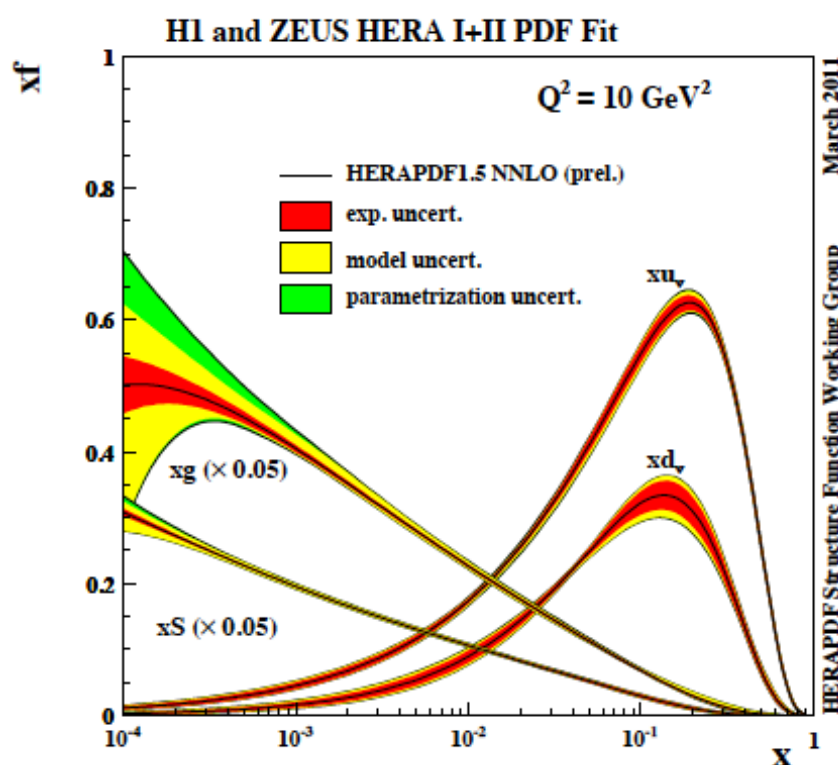
In DIS the inclusive cross section depends on two variables, the negative 4-momentum transfer squared (Q^2), which determines the resolving power of the exchanged particle in terms of p substructure, and the variable Bjorken x, which Feynman could relate to the fraction of momentum of the proton carried by a parton [in what he called the 'infinite momentum frame' in which the transverse momenta are neglected].

Feynman's partons were readily linked to Gell-Mann and Zweig's quarks.

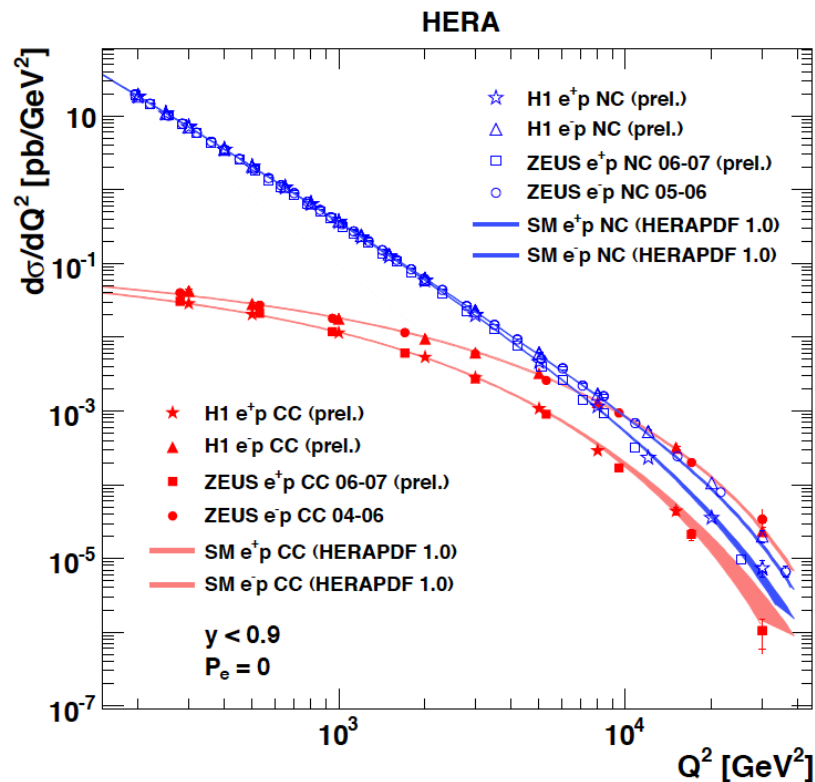
This process has been for 20 years recently been investigated at HERA.

**Deep inelastic scattering resolves the nucleon structure. If s is high: produce new states
Kinematics is determined with scattered electron or with HFS → high precision due to redundancy**

Results from HERA



F_2 rises towards low x , and xg too.
Parton evolution - QCD to NNLO



The weak and electromagnetic interactions reach similar strength when $Q^2 \geq M_{W,Z}^2$

Measurements on α_s , Basic tests of QCD: longitudinal structure function, jet production, γ structure
Some 10% of the cross section is diffractive ($ep \rightarrow eXp$) : diffractive partons; c,b quark distributions
New concepts: unintegrated parton distributions (k_T), generalised parton distributions (DVCS)
New limits for leptoquarks, excited electrons and neutrinos, quark substructure, RPV SUSY
Interpretation of the Tevatron measurements (high E_T jet excess, M_W , searches..)

What HERA could not do or has not done

HERA in one box
the first ep collider

$E_p * E_e =$
 $920 * 27.6 \text{ GeV}^2$
 $\sqrt{s} = 2\sqrt{E_e E_p} = 320 \text{ GeV}$

$L = 1..4 \cdot 10^{31} \text{ cm}^{-2} \text{s}^{-1}$
 $\rightarrow \Sigma L = 0.5 \text{ fb}^{-1}$
1992-2000 & 2003-2007

$Q^2 = [0.1 -- 3 * 10^4] \text{ GeV}^2$
-4-momentum transfer²

$x = Q^2 / (s y) \approx 10^{-4} .. 0.7$
Bjorken x

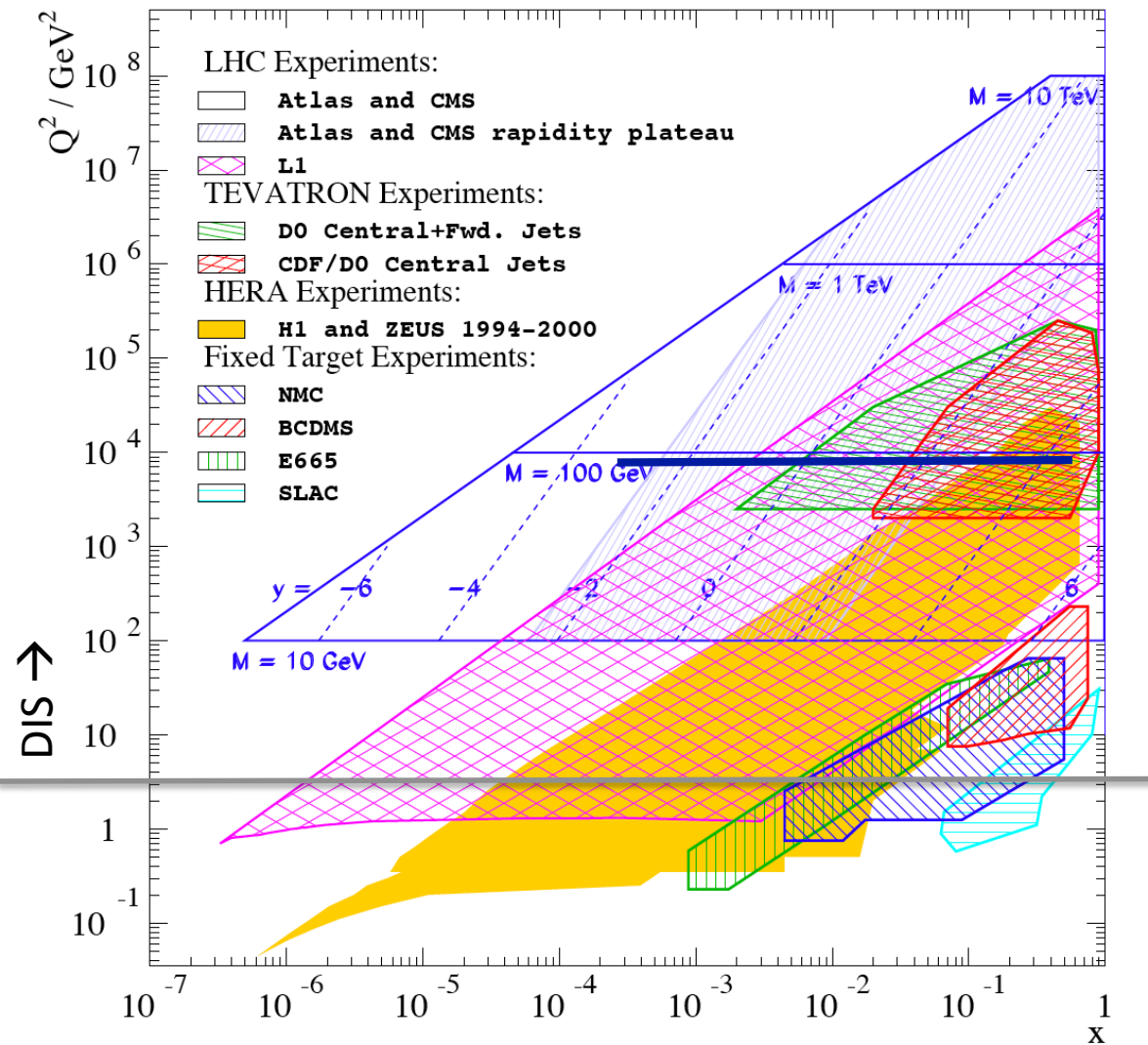
$y \approx 0.005 .. 0.9$
inelasticity

Test of the isospin symmetry (u-d) with eD - no deuterons
Investigation of the q-g dynamics in nuclei - no time for eA
Verification of saturation prediction at low x – too low s
Measurement of the strange quark distribution – too low L
Discovery of Higgs in WW fusion in CC – too low cross section
Study of top quark distribution in the proton – too low s
Precise measurement of F_L – too short running time left
Resolving d/u question at large Bjorken x – too low L
Determination of gluon distribution at hi/lo x – too small range
High precision measurement of α_s – overall not precise enough
Discovering instantons, odderons – don't know why not
Finding RPV SUSY and/or leptoquarks – may reside higher up
...

The H1 and ZEUS apparatus were basically well suited
The machine had too low luminosity and running time

HEP needs a TeV energy scale machine with 100 times higher luminosity than HERA to develop DIS physics further and to complement the physics at the LHC. The Large Hadron Collider p and A beams offer a unique opportunity to build a second ep and first eA collider at the energy frontier.

Complementing the LHC with ep/A



LHC partons: W,Z +c,b new constraints
but severely limited in x,Q^2 range

Discoveries at the LHC will be at high masses: large x and very high Q^2
which require high s , lumi of LHeC
for precision PDFs (u,d,xg mainly)

If the Higgs exists, its study will
become a major field of research:
ep: $WW \rightarrow H \rightarrow b\bar{b}$ (CP odd/even?)

top distribution in the proton TDF

IF RP is violated and LQ or RPV SUSY
discovered: LHeC is uniquely suited

AA: QGP: study initial state in eA
Resolve parton distributions in nuclei

LHeC is unique in various areas, e.g.:
Low x and saturation physics
Strong coupling constant to 0.1% level

II Physics

4 Precision QCD and Electroweak Physics

- 4.1 Inclusive Deep Inelastic Scattering
 - 4.1.1 Cross Sections and Structure Functions
 - 4.1.2 Neutral Current
 - 4.1.3 Charged Current
 - 4.1.4 Cross Section Simulation and Uncertainties
 - 4.1.5 Longitudinal Structure Function F_L
 - 4.2 Determination of Parton Distributions
 - 4.2.1 QCD Fit Ansatz
 - 4.2.2 Valence Quarks
 - 4.2.3 Strange Quarks
 - 4.2.4 Top Quarks
 - 4.3 Gluon Distribution
 - 4.4 Prospects to Measure the Strong Coupling Constant
 - 4.4.1 Status of the DIS Measurements of α_s
 - 4.4.2 Simulation of α_s Determination
 - 4.5 Electron-Deuteron Scattering
 - 4.6 Charmed and Beauty production
 - 4.6.1 Introduction and overview of expected highlights
 - 4.6.2 Total production cross sections for charm, beauty and top quarks
 - 4.6.3 Charm and Beauty production in DIS
 - 4.6.4 Intrinsic Heavy Flavour
 - 4.6.5 D^* meson photoproduction study
 - 4.7 High p_T jets
 - 4.7.1 Jets in ep
 - 4.7.2 Jets in γA
 - 4.8 Total photoproduction cross section
 - 4.9 Electroweak physics
 - 4.9.1 The context
 - 4.9.2 Light Quark Weak Neutral Current Couplings
 - 4.9.3 Determination of the Weak Mixing Angle
- 153 pages**
- now
- then

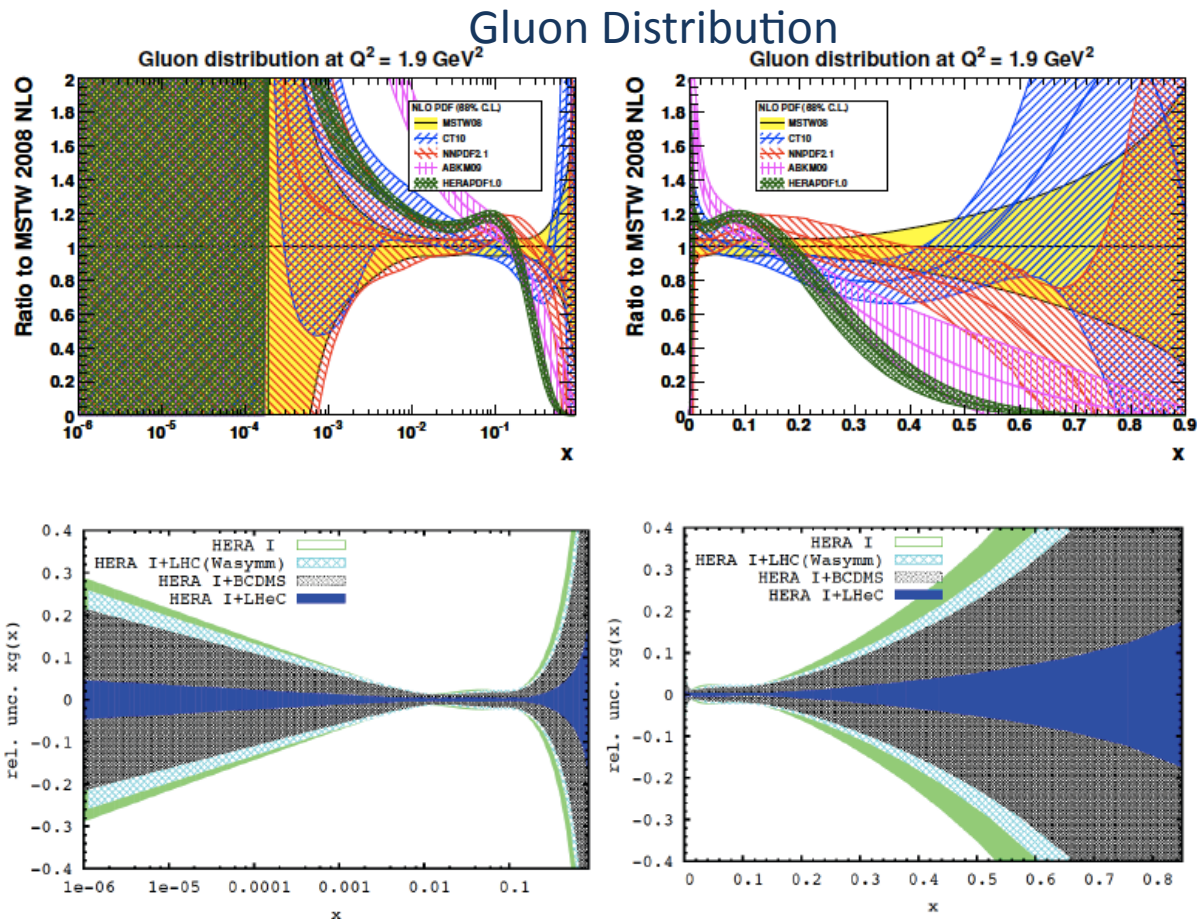


Figure 4.17: Relative uncertainty of the gluon distribution at $Q^2 = 1.9 \text{ GeV}^2$, as resulting from an NLO QCD fit to HERA (I) alone (green, outer), HERA and BCDMS (crossed), HERA and LHC (light blue, crossed) and the LHeC added (blue, dark). Left: logarithmic x , right: linear x .

Precision measurement of gluon density to extreme $x \rightarrow \alpha_s$

Low x : saturation in ep ? Crucial for QCD, LHC, UHE neutrinos!

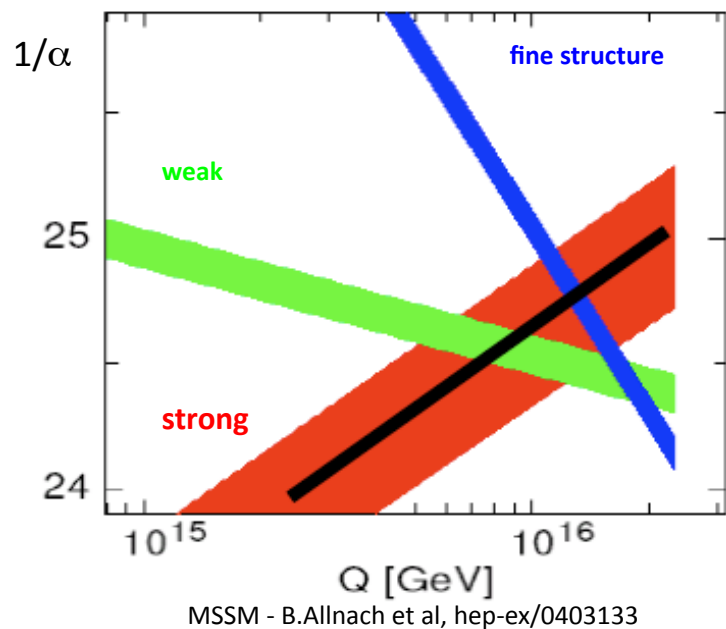
High x : xg and valence quarks: resolving new high mass states!

Gluon in Pomeron, odderon, photon, nuclei.. Local spots in p ?

Heavy quarks intrinsic or only gluonic?

Strong Coupling Constant

Simulation of α_s measurement at LHeC



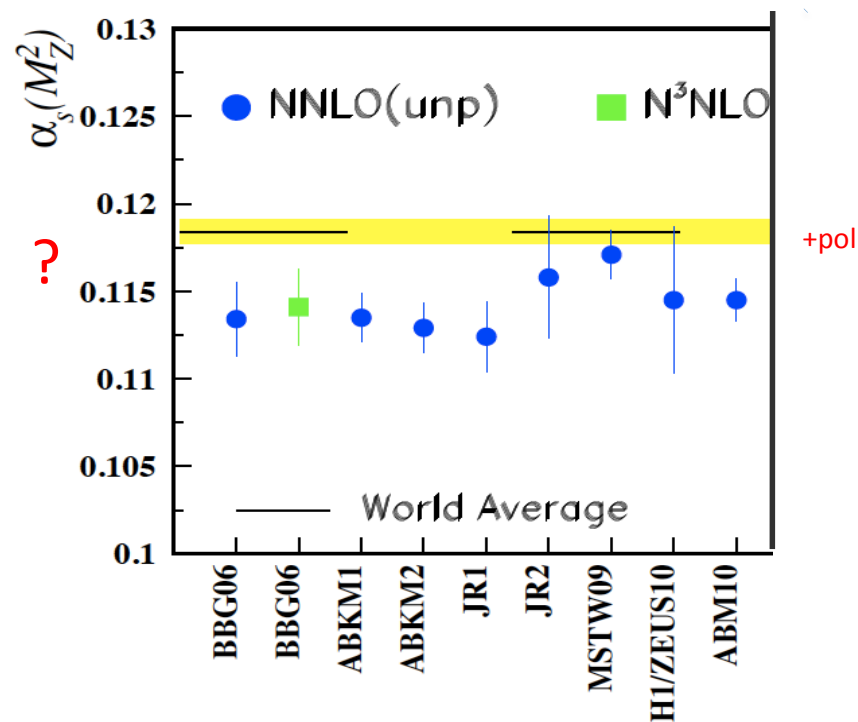
<u>DATA</u>	<u>exp. error on α_s</u>
NC e ⁺ only	0.48%
NC	0.41%
NC & CC	0.23% :=⁽¹⁾
⁽¹⁾ $\gamma_h > 5^\circ$	0.36% := ⁽²⁾
⁽¹⁾ +BCDMS	0.22%
⁽²⁾ +BCDMS	0.22%
⁽¹⁾ stat. *= 2	0.35%

Two independent analyses performed

α_s least known of coupling constants
Grand Unification predictions suffer from $\delta\alpha_s$

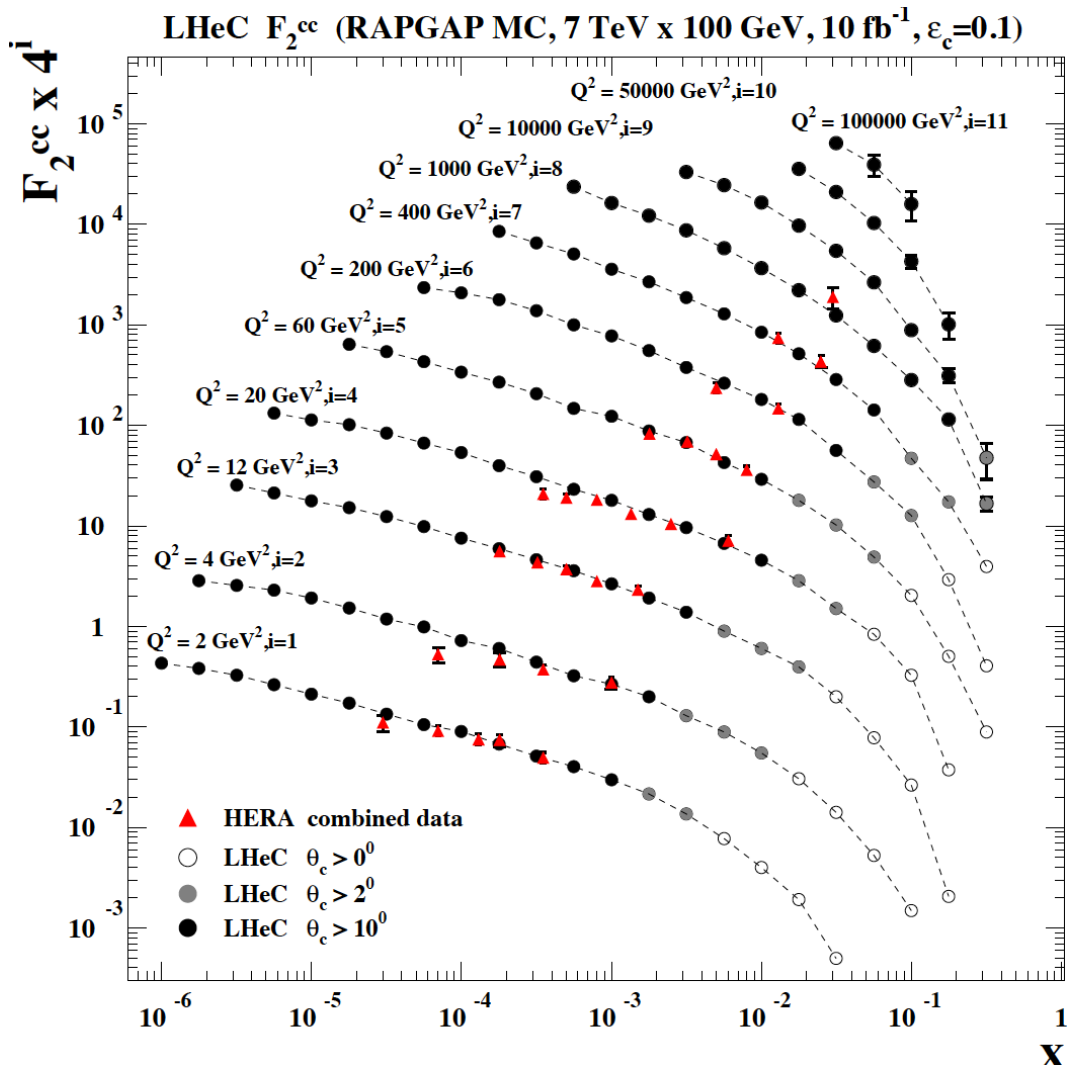
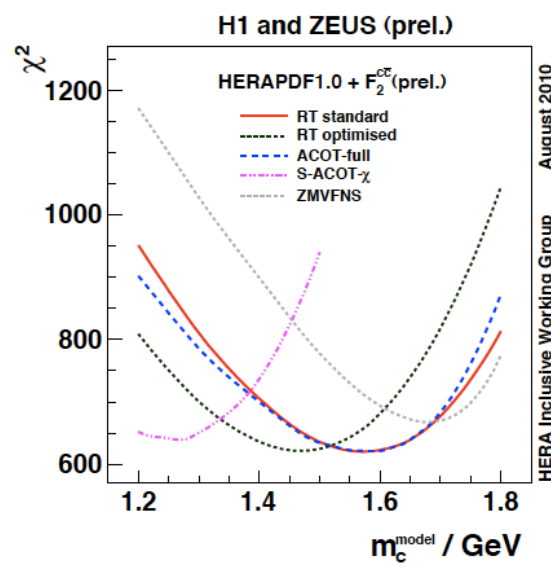
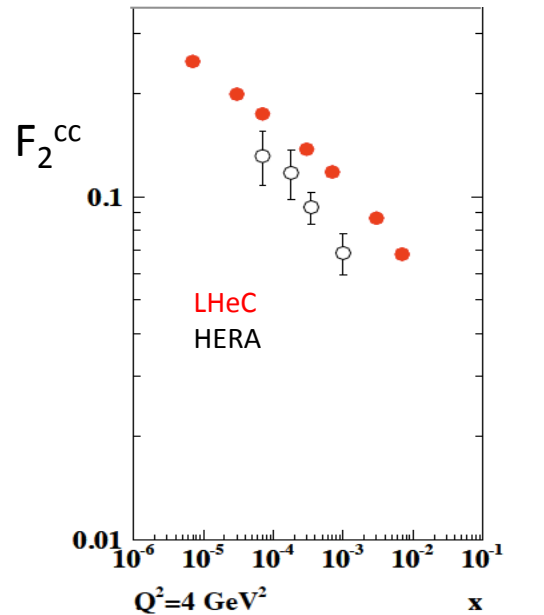
DIS tends to be lower than world average
Recently challenged by MSTW and NNPDF – jets??

LHeC: per mille accuracy - independent of BCDMS.
Challenge to experiment and to h.o. QCD →
A genuine DIS research programme rather than
one outstanding measurement only.



J.Bluemlein and H. Boettcher, arXiv 1005.3013 (2010)

Treatment of charm influences α_s

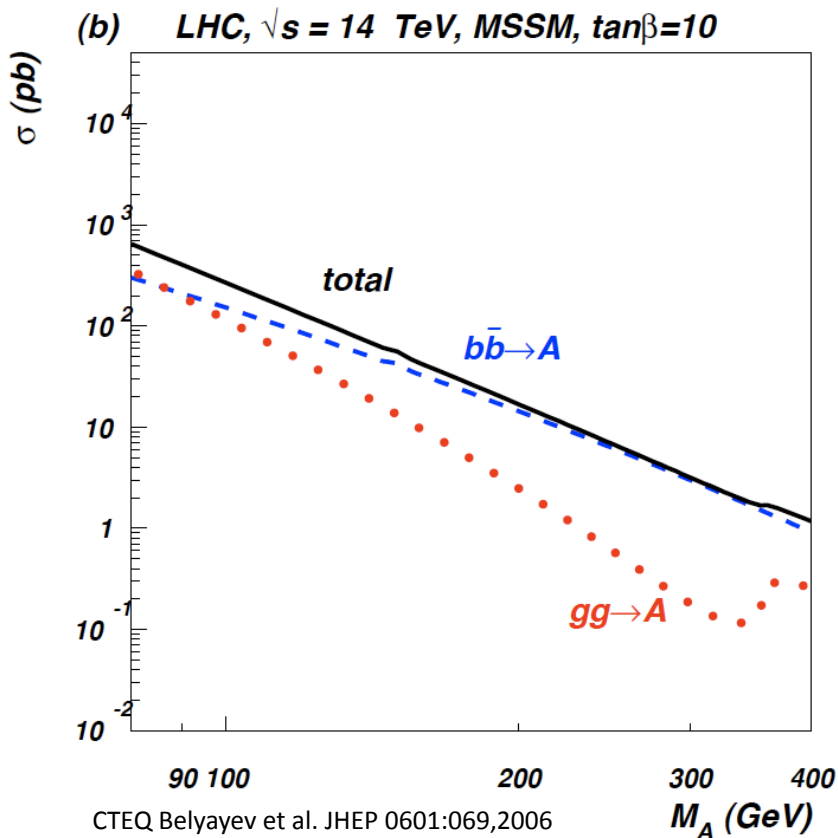


LHeC vs HERA: higher fraction of c, larger range, smaller beam spot, better Silicon detectors

note: 100 MeV of m_c is about 1% on α_s

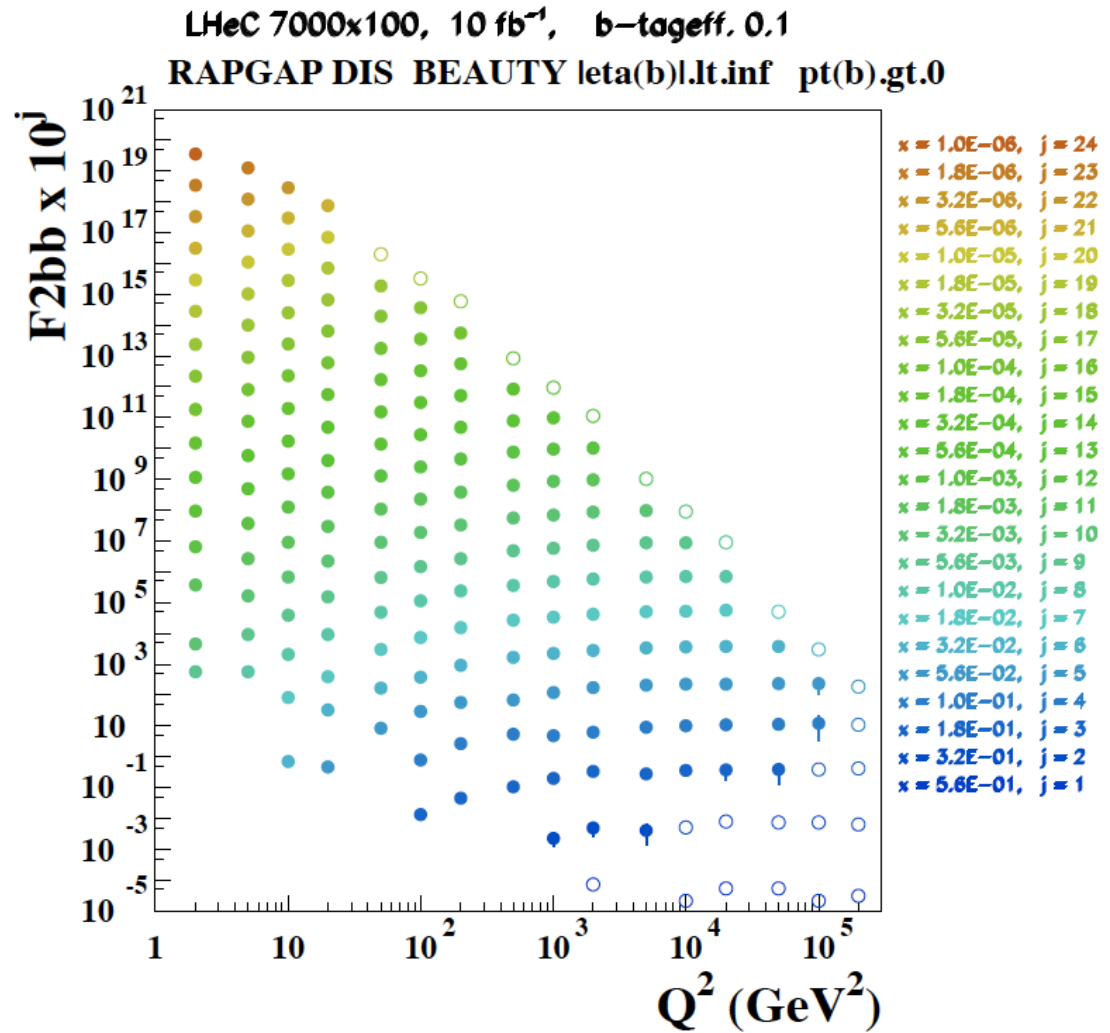
CDR

Beauty - MSSM Higgs



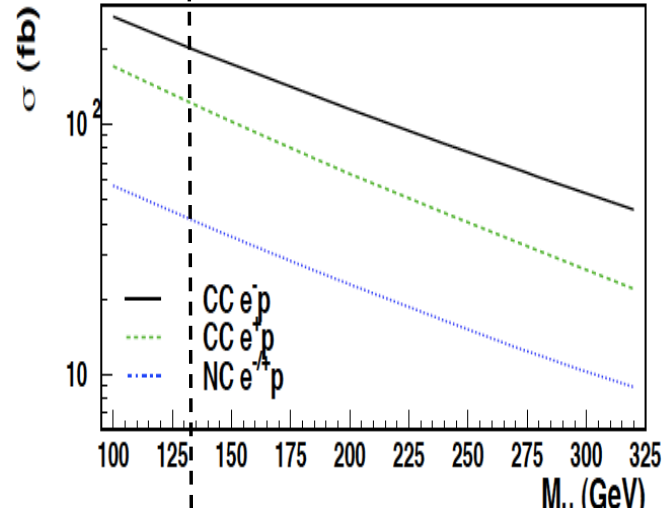
In MSSM Higgs production is b dominated

HERA: First measurements of b to $\sim 20\%$
LHeC: precision measurement of b-df

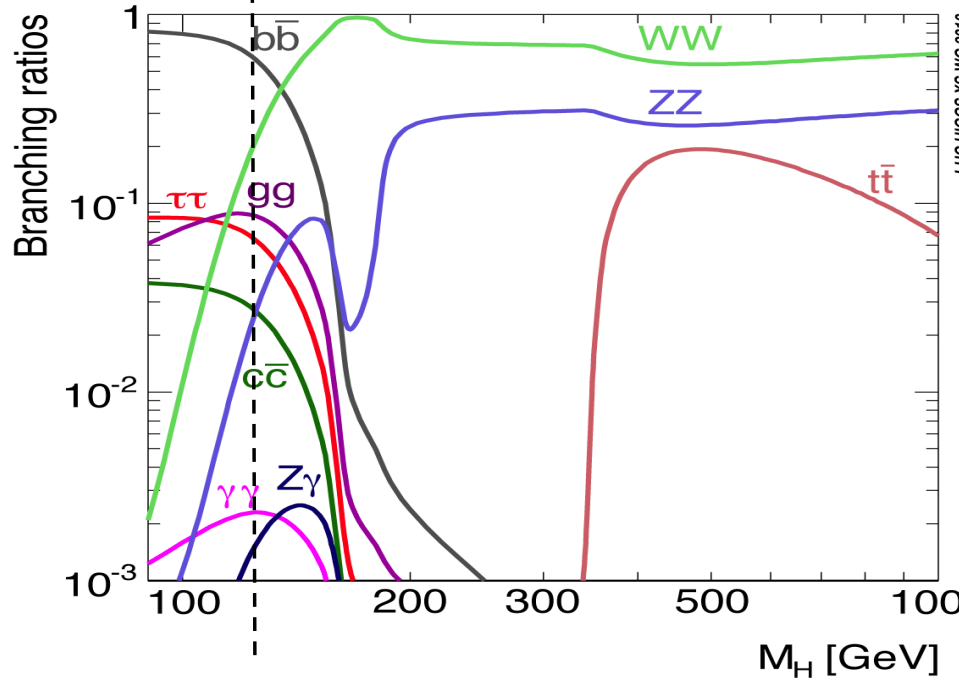
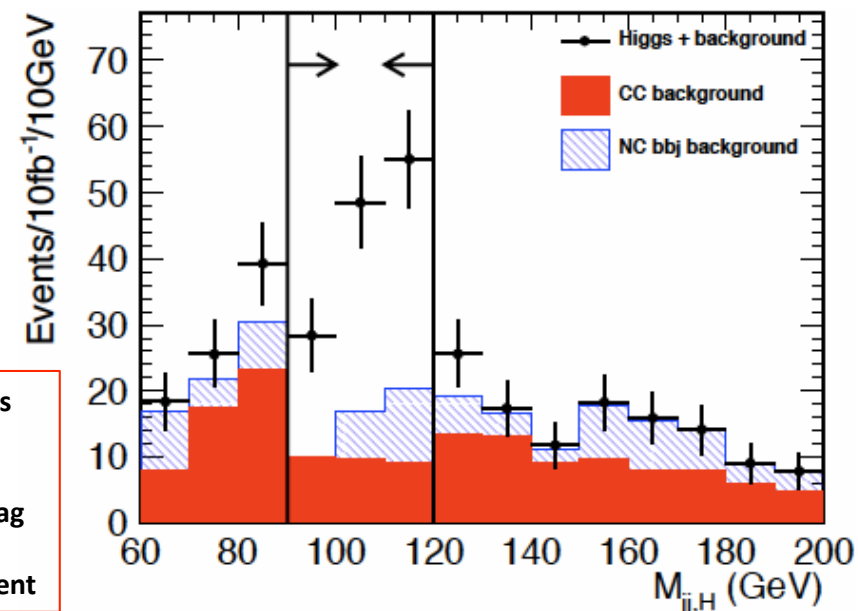


LHeC: higher fraction of b, larger range,
smaller beam spot, better Si detectors

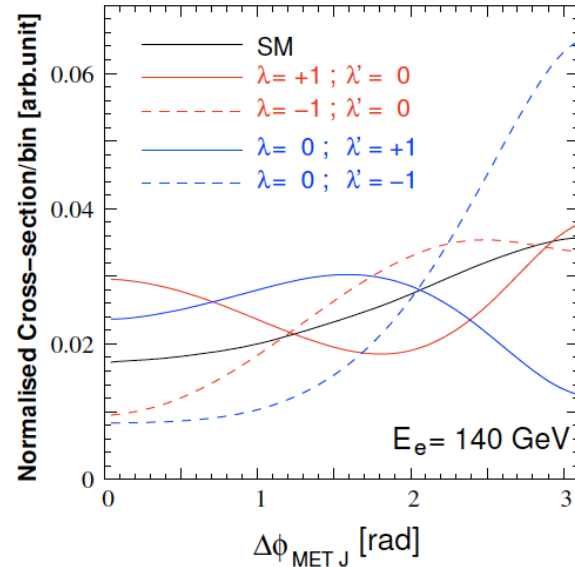
Higgs



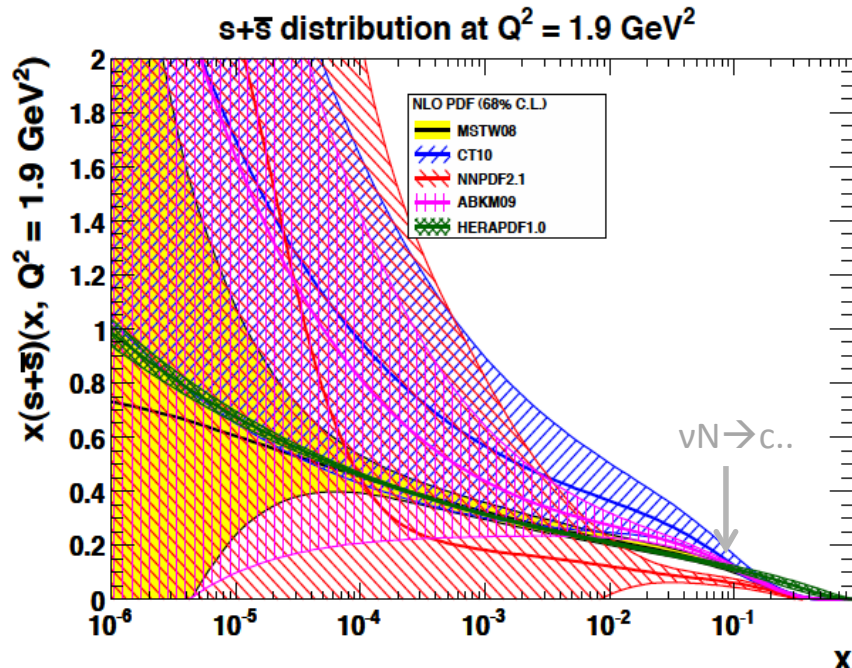
Process determines much of detector acceptance and calibration and b tag (also single top) and L/ E_e requirement



Higgs is light (or absent), CC: $WW \rightarrow H \rightarrow bb$
CP even: SM, CP odd: nonSM, mixture?



Strange and Valence Quarks

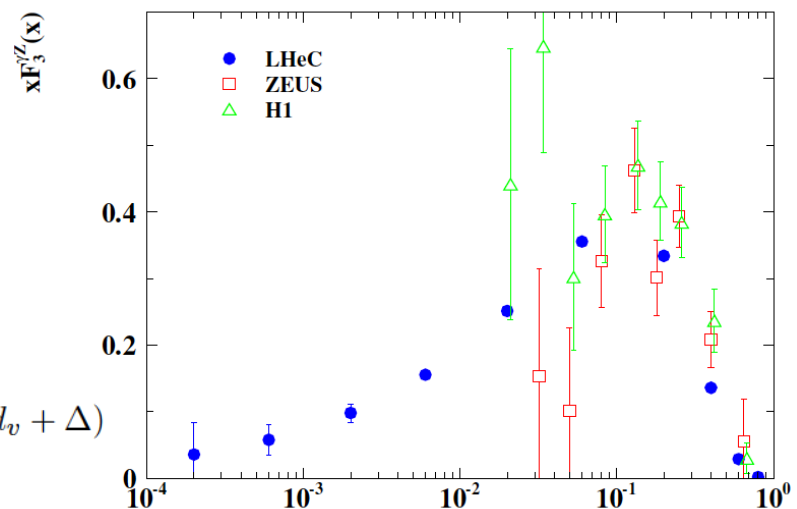
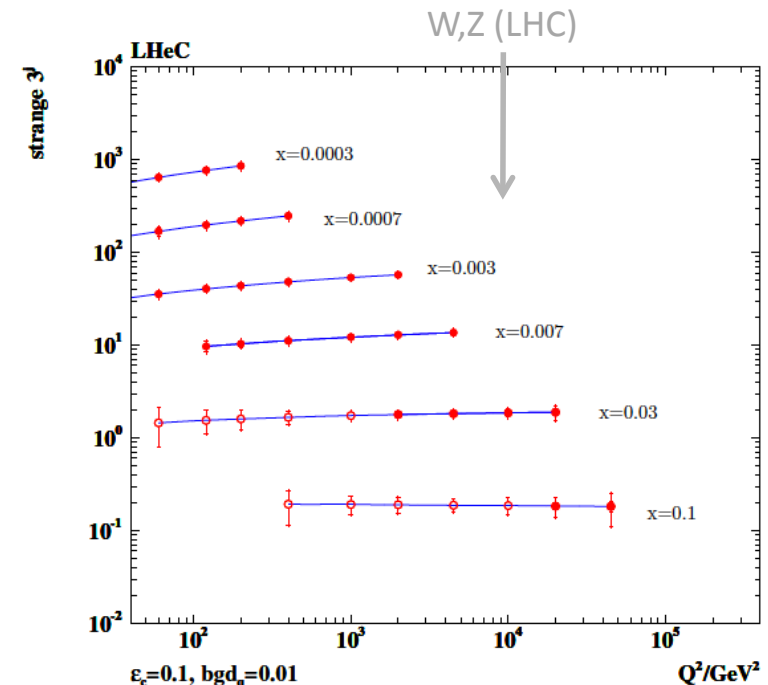


Strange quark density unknown
at low x and controversial at high $x \sim 0.1$

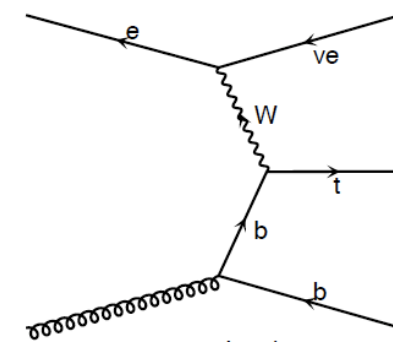
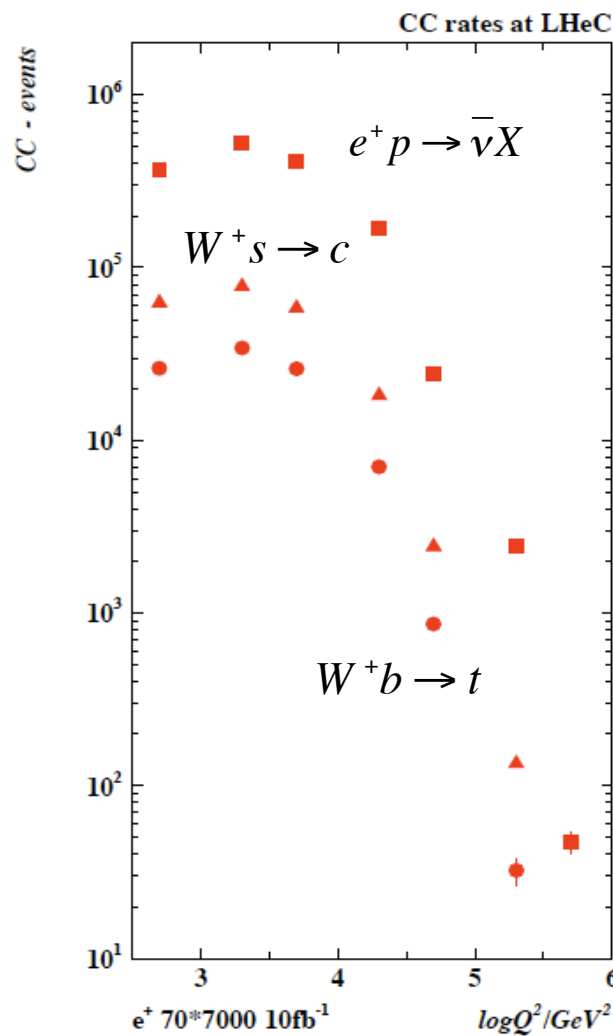
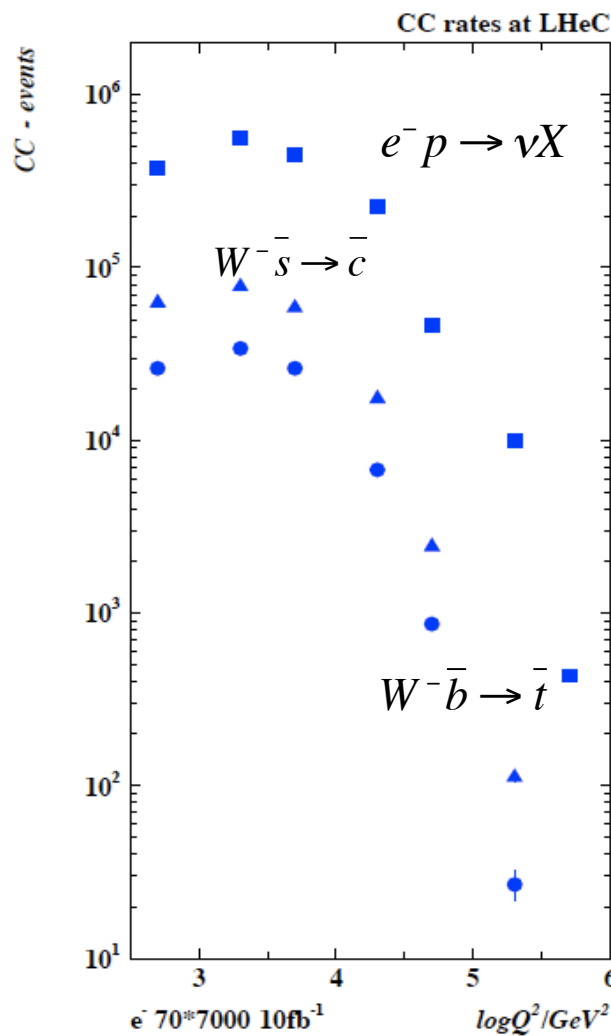
Low x sea to be unfolded with LHeC
CC and ep and eD measurements
down to $x=10^{-4..6}$

$$xF_3^{\gamma Z} = \frac{x}{3}(2u_v + d_v + \Delta)$$

Sea Quarks=Antiquarks? Need u_v, d_v



$\overline{\text{Top}}$ and Top Production in Charged Currents



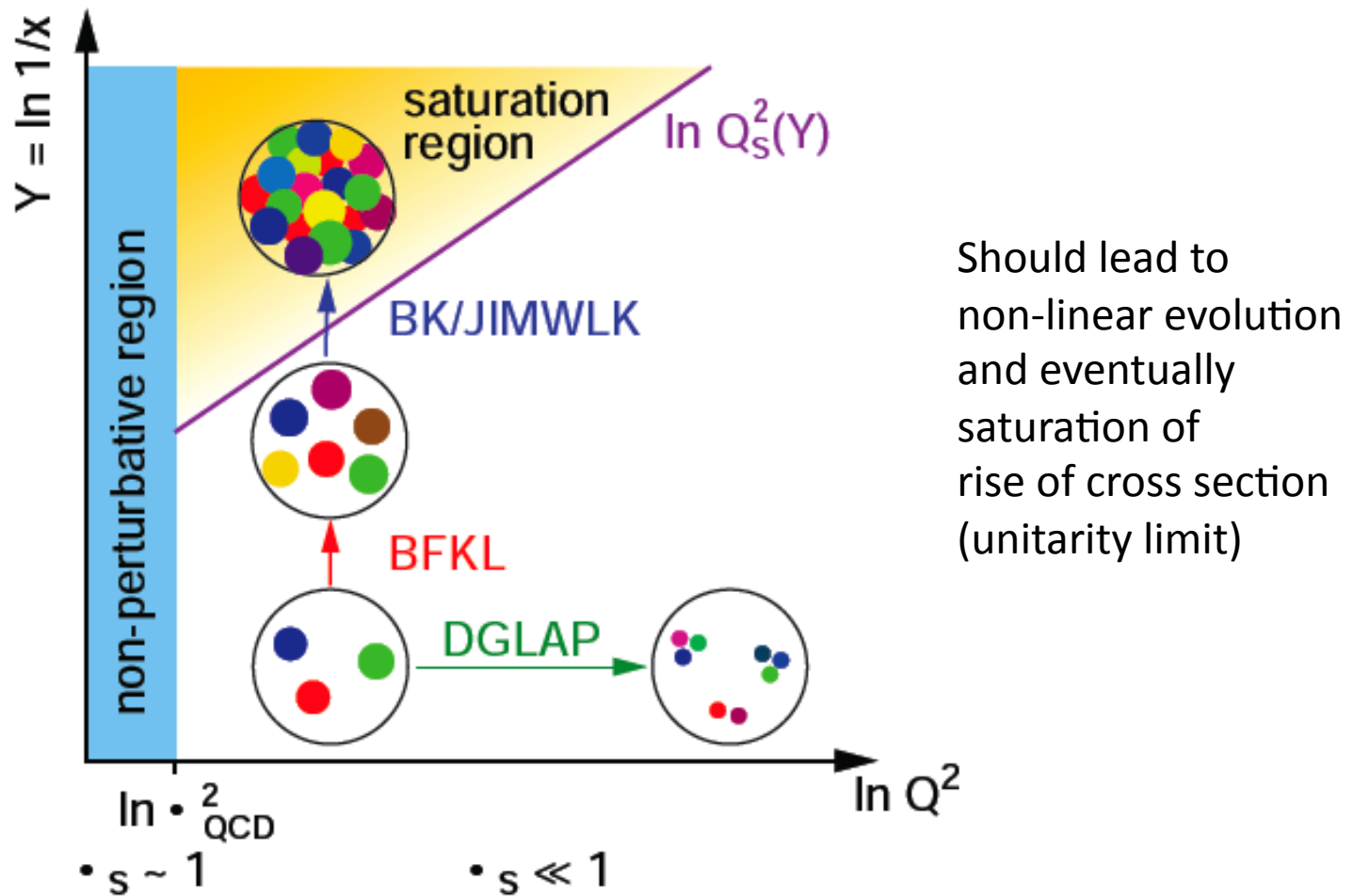
LHeC copious
single top and anti-top
quark production

with a CC cross section
of $O(10)$ pb

Study Q^2 evolution of
top quark onset –
6 quark CFNS
(Pascaud at DIS11)

m_{top}
Not yet simulated..

High Parton Densities

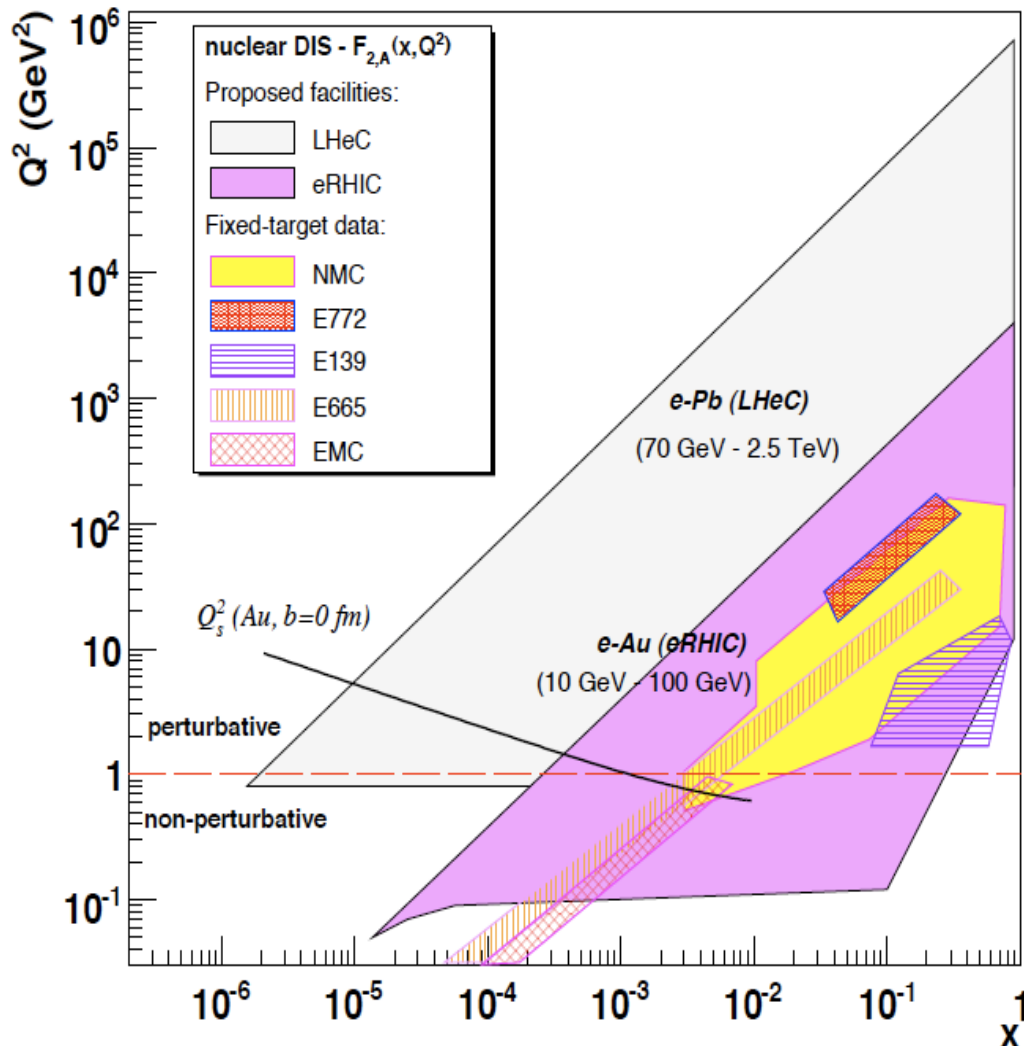


CDR $L_{eN} \approx 3 * 10^{31} \text{ cm}^{-2}\text{s}^{-1}$ for D,A - not optimised

The study of deep inelastic ep scattering is important for the investigation of the nature of the Pomeron and Odderon, which are Regge singularities of the t -channel partial waves $f_j(t)$ in the complex plane of the angular momentum j . The Pomeron is responsible for a growth of total cross sections with energy. The Odderon describes the behaviour of the difference of the cross sections for particle-particle and particle-antiparticle scattering which obey the Pomeranchuk theorem. In perturbative QCD, the Pomeron and Odderon are the simplest colorless reggeons (families of glueballs) constructed from two and three reggeized gluons, respectively. Their wave functions satisfy the generalized BFKL equation. In the next-to-leading approximation the solution of the BFKL equation contains an infinite number of Pomerons and to verify this prediction of QCD one needs to increase the energy of colliding particles. In the $N=4$ supersymmetric generalization of QCD, in the t'Hooft limit of large N_c , the BFKL Pomeron is equivalent to the reggeized graviton living in the 10-dimensional anti-de-Sitter space. Therefore, the Pomeron interaction describing the screening corrections to the BFKL predictions, at least in this model, should be based on a general covariant effective theory being a generalization of the Einstein-Hilbert action for general relativity. Thus, the investigation of high energy ep scattering could be interesting for the construction of a non-perturbative approach to QCD based on an effective string model in high dimensional spaces.

Lev Lipatov in the CDR...

Electron-Ion Scattering



EIC programme:
see recent workshop arXiv:1108.1713 [nucl-th]

Dipole models predict **saturation** which resummation in pQCD moves to lower x..

It requires highest energy, low x, $Q^2 > M_p^2$

Saturation at the LHeC is predicted to be observed both in ep AND in eA.

This combination is crucial to disentangle nuclear from unitarity effects.

Expect **qualitative changes of behaviour**

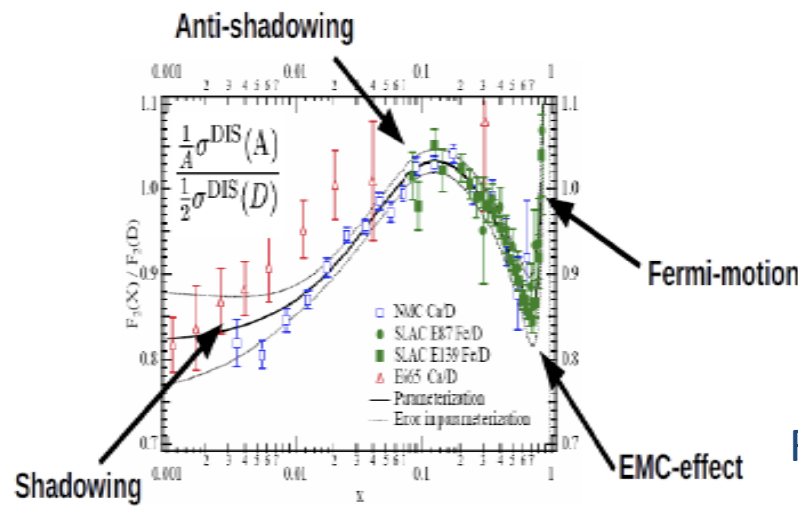
- Black body limit of F_2
- Saturation amplified with $A^{1/3}$
- Rise of diffraction to 50%?

Below $x \sim 10^{-2}$: DIS data end. NO flavour separation yet. However indications are that e.g. shadowing is flavour dependent.

Deuterons: tag spectator,
relate shadowing-diffraction (Gribov)!
stabilise QCD evolution (singlet!)

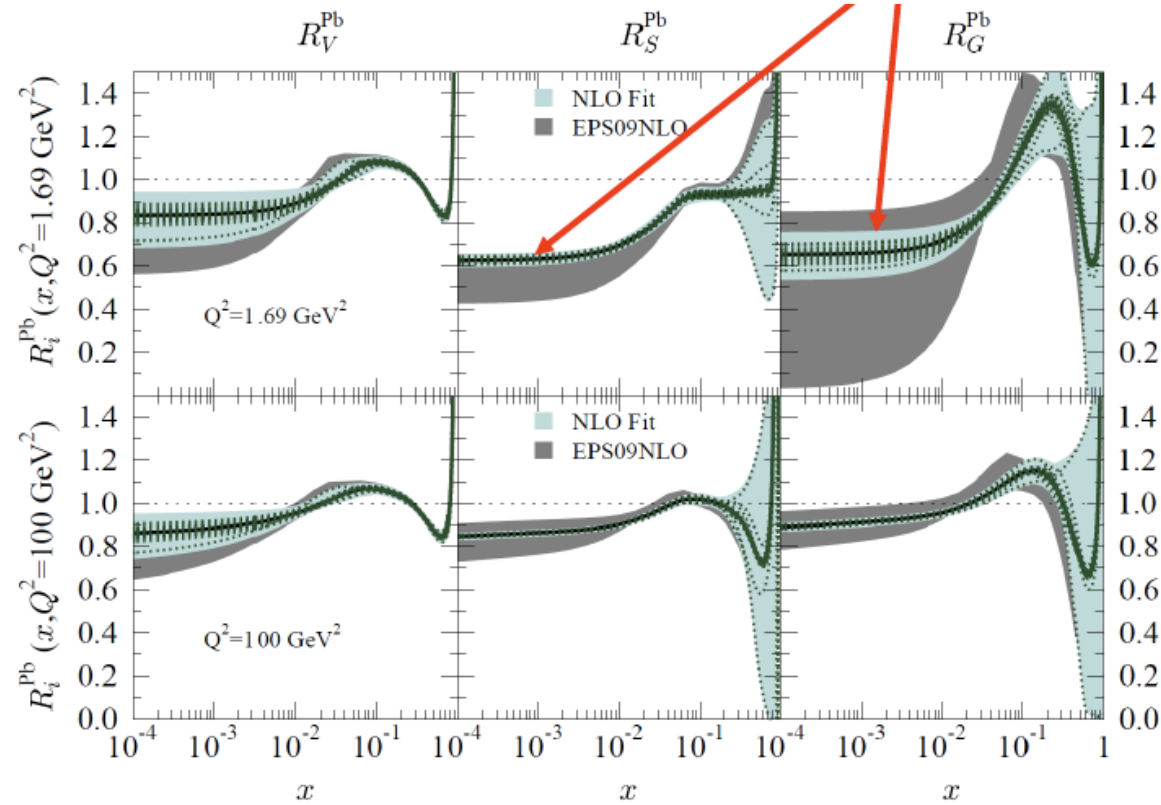
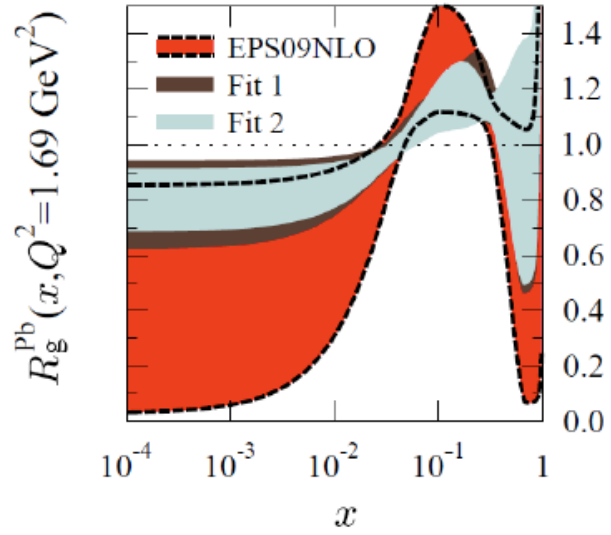
Neutron (light sea, UHE neutrinos, QPM)

Nuclear Parton Distributions



Study using eA LHeC pseudodata

$R = q^{\text{Pb}}/q^{\text{p}}$

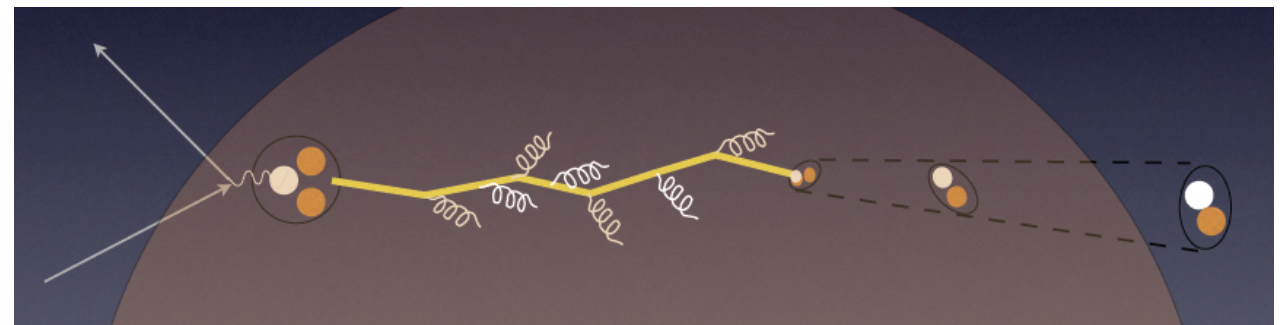


→ A complete determination of nPDFs in grossly extended range, into nonlinear regime certainly more diverse than in V,S,G terms and cleaner than pA at the LHC

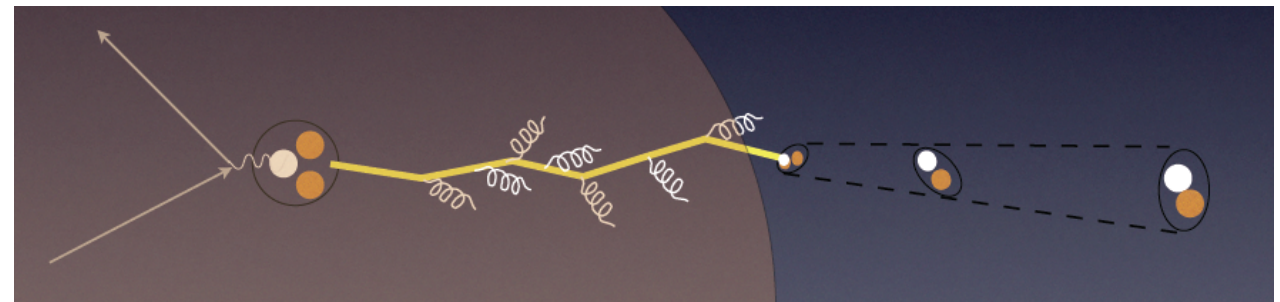
In-medium Hadronisation

The study of particle production in eA (fragmentation functions and hadrochemistry) allows the study of the space-time picture of hadronisation (the final phase of QGP).

Low energy (ν): need of hadronization inside.
Parton propagation: pt broadening
Hadron formation: attenuation



High energy (ν): partonic evolution altered in the nuclear medium.

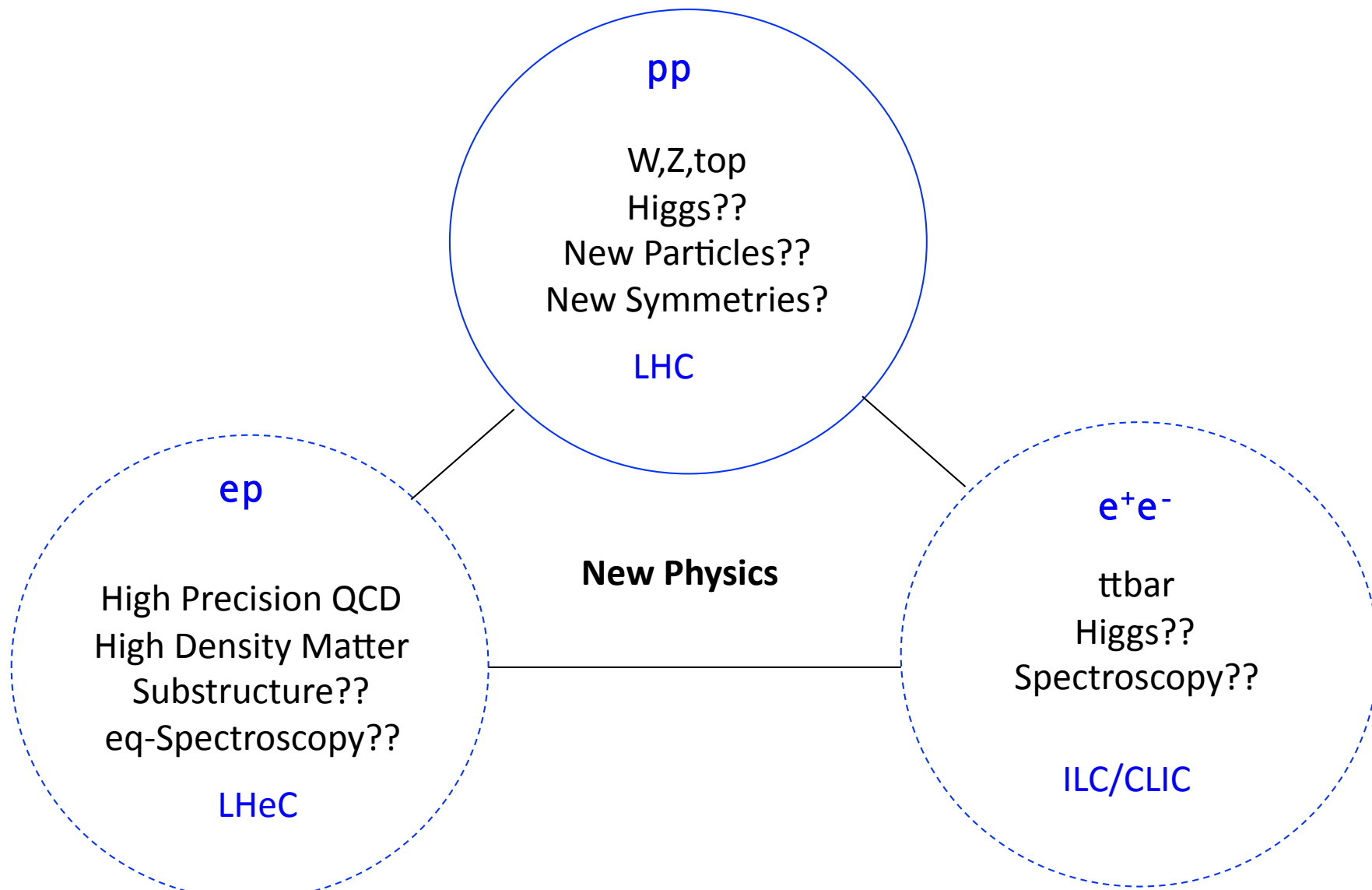


W.Brooks, Divonne09

LHeC :

- + study the transition from small to high energies in much extended range wrt. fixed target data
- + testing the energy loss mechanism crucial for understanding of the medium produced in HIC
- + detailed study of heavy quark hadronisation ...

The TeV Scale [2010-2035..]



II. Accelerator and Detector

LHeC Accelerator Design: Participating Institutes



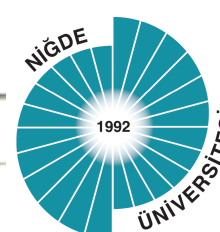
The Cockcroft Institute
of Accelerator Science and Technology



Norwegian University of
Science and Technology



ANKARA ÜNİVERSİTESİ



TOBB ETU



Laboratori Nazionali di Legnaro



Physique des accélérateurs



ÉCOLE POLYTECHNIQUE
FÉDÉRALE DE LAUSANNE



UNIVERSITY OF
LIVERPOOL



Electron Beam -Two Options

$$L = \frac{N_p \gamma}{4\pi e \varepsilon_{pn}} \cdot \frac{I_e}{\sqrt{\beta_{px} \beta_{py}}}$$

$$N_p = 1.7 \cdot 10^{11}, \varepsilon_p = 3.8 \mu m, \beta_{px(y)} = 1.8(0.5)m, \gamma = \frac{E_p}{M_p}$$

$$L = 8.2 \cdot 10^{32} cm^{-2}s^{-1} \cdot \frac{N_p 10^{-11}}{1.7} \cdot \frac{m}{\sqrt{\beta_{px} \beta_{py}}} \cdot \frac{I_e}{50mA}$$

$$I_e = 0.35mA \cdot P[MW] \cdot (100/E_e[GeV])^4$$

Ring-Ring

Power Limit of 100 MW wall plug
 “ultimate” LHC proton beam
60 GeV e \pm beam

$$\rightarrow L = 2 \cdot 10^{33} \text{ cm}^{-2}\text{s}^{-1} \rightarrow O(100) \text{ fb}^{-1}$$

LINAC Ring

Pulsed, **60 GeV**: $\sim 10^{32}$

High luminosity:

Energy recovery: $P = P_0 / (1 - \eta)$

$\beta^* = 0.1m$

[5 times smaller than LHC by reduced Γ^* , only one p squeezed and IR quads as for HL-LHC]

$$L = 10^{33} \text{ cm}^{-2}\text{s}^{-1} \rightarrow O(100) \text{ fb}^{-1}$$

$$L = \frac{1}{4\pi} \cdot \frac{N_p}{\varepsilon_p} \cdot \frac{1}{\beta^*} \cdot \gamma \cdot \frac{I_e}{e}$$

$$N_p = 1.7 \cdot 10^{11}, \varepsilon_p = 3.8 \mu m, \beta^* = 0.2m, \gamma = 7000/0.94$$

$$L = 8 \cdot 10^{31} cm^{-2}s^{-1} \cdot \frac{N_p 10^{-11}}{1.7} \cdot \frac{0.2}{\beta^*/m} \cdot \frac{I_e / mA}{1}$$

$$I_e = mA \frac{P / MW}{E_e / GeV}$$

Synchronous ep and pp operation (small ep tuneshifts)

The LHC p beams provide 100 times HERA's luminosity

e Ring- p/A Ring

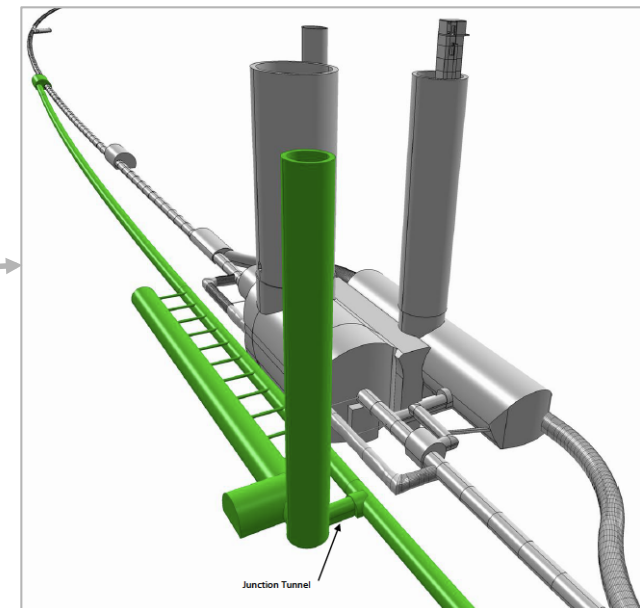
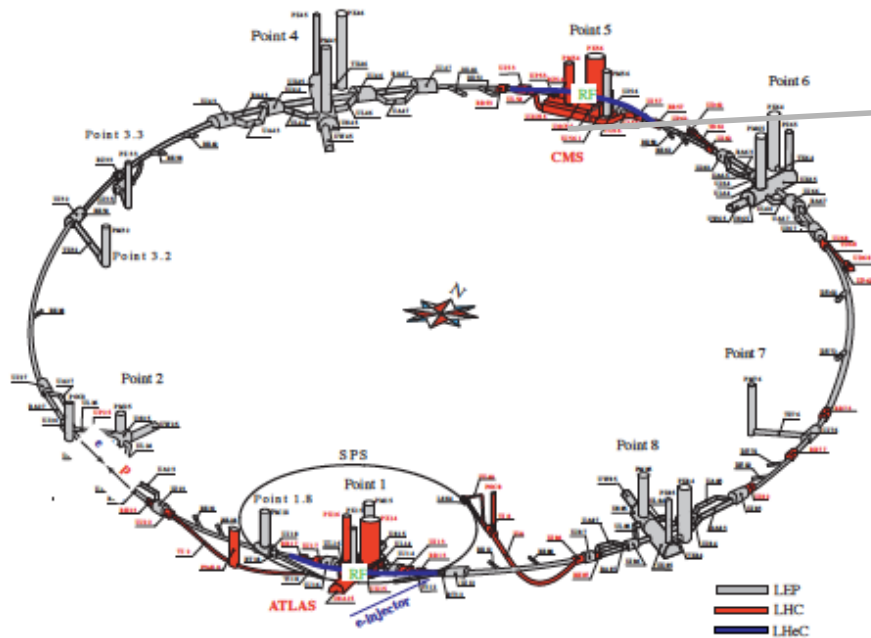
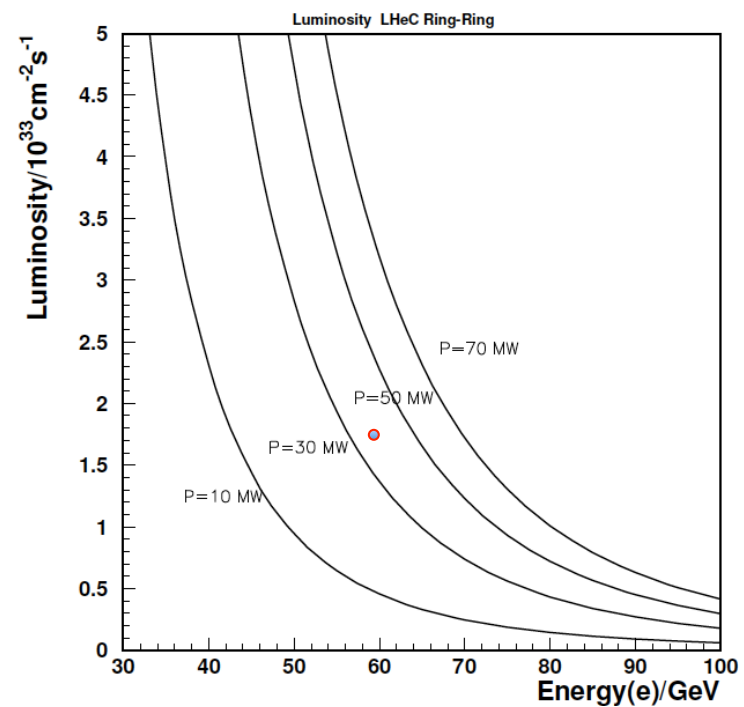
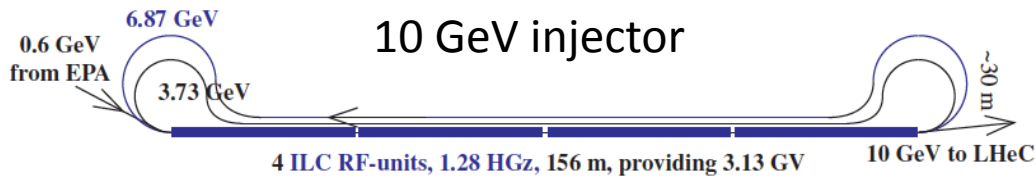
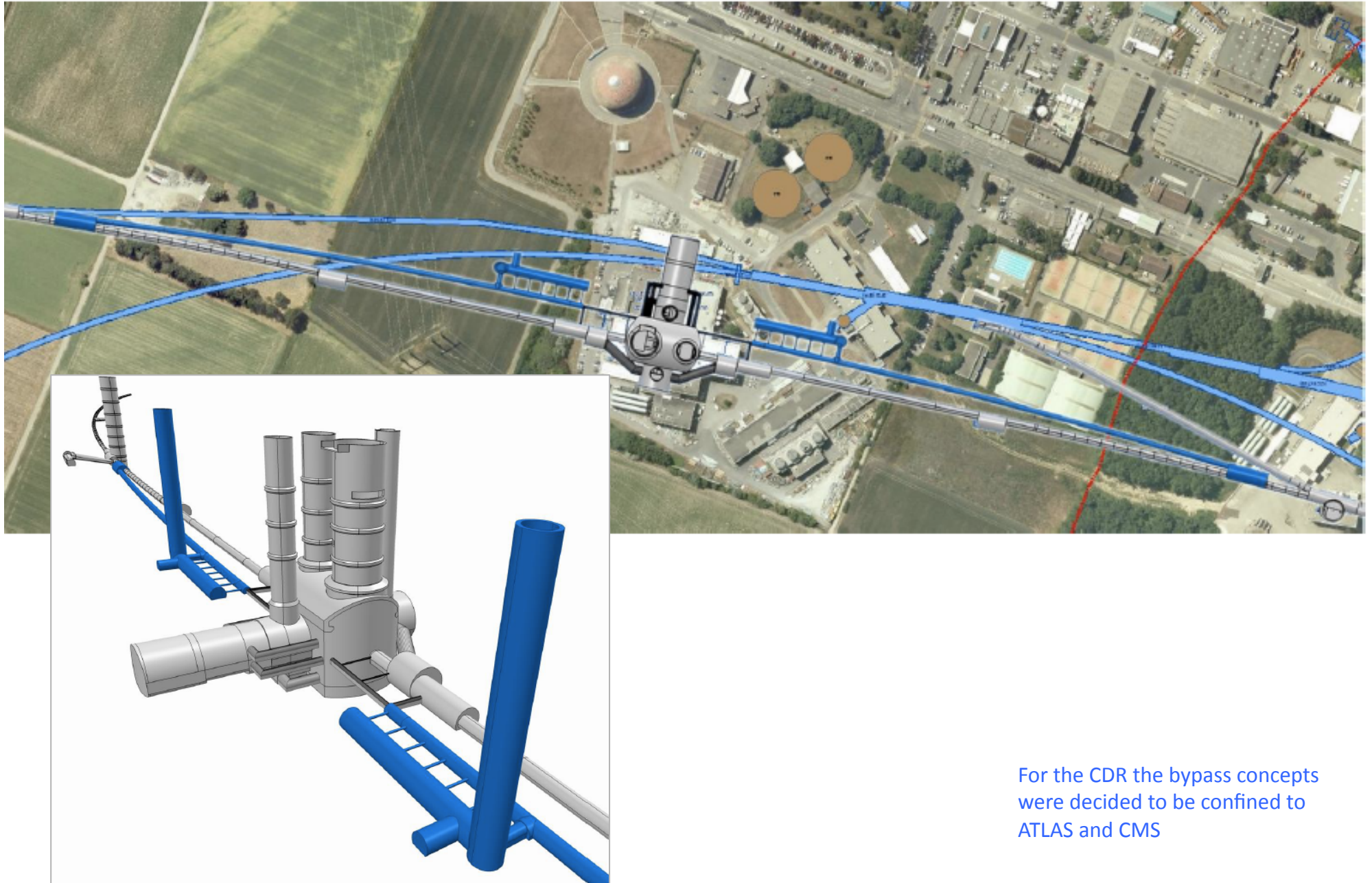


Figure 1: Schematic Layout of the LHC (grey/red) with the bypasses of CMS and ATLAS for the ring electron beam (blue) in the RR version. The e injector is a 10 GeV superconducting linac in triple racetrack configuration which is considered to reach the ring via the bypass around ATLAS.



Bypassing ATLAS



For the CDR the bypass concepts
were decided to be confined to
ATLAS and CMS

Magnets

9 System Design

9.1	Magnets for the Interaction Region
9.1.1	Introduction
9.1.2	Magnets for the ring-ring option
9.1.3	Magnets for the linac-ring option
9.2	Accelerator Magnets
9.2.1	Dipole Magnets
9.2.2	BINP Model
9.2.3	CERN Model
9.2.4	Quadrupole and Corrector Magnets
9.3	Ring-Ring RF Design
9.3.1	Design Parameters
9.3.2	Cavities and klystrons
9.4	Linac-Ring RF Design
9.4.1	Design Parameters
9.4.2	Layout and RF powering
9.4.3	Arc RF systems
9.5	Crab crossing for the LHeC
9.5.1	Luminosity Reduction
9.5.2	Crossing Schemes
9.5.3	RF Technology
9.6	Vacuum
9.6.1	Vacuum requirements
9.6.2	Synchrotron radiation
9.6.3	Vacuum engineering issues
9.7	Beam Pipe Design
9.7.1	Requirements
9.7.2	Choice of Materials for beampipes
9.7.3	Beampipe Geometries
9.7.4	Vacuum Instrumentation
9.7.5	Synchrotron Radiation Masks
9.7.6	Installation and Integration
9.8	Cryogenics
9.8.1	Ring-Ring Cryogenics Design
9.8.2	Linac-Ring Cryogenics Design
9.8.3	General Conclusions Cryogenics for LHeC
9.9	Beam Dumps and Injection Regions
9.9.1	Injection Region Design for Ring-Ring Option
9.9.2	Injection transfer line for the Ring-Ring Option
9.9.3	60 GeV internal dump for Ring-Ring Option
9.9.4	Post collision line for 140 GeV Linac-Ring option
9.9.5	Absorber for 140 GeV Linac-Ring option
9.9.6	Energy deposition studies for the Linac-Ring option
9.9.7	Beam line dump for ERL Linac-Ring option
9.9.8	Absorber for ERL Linac-Ring option

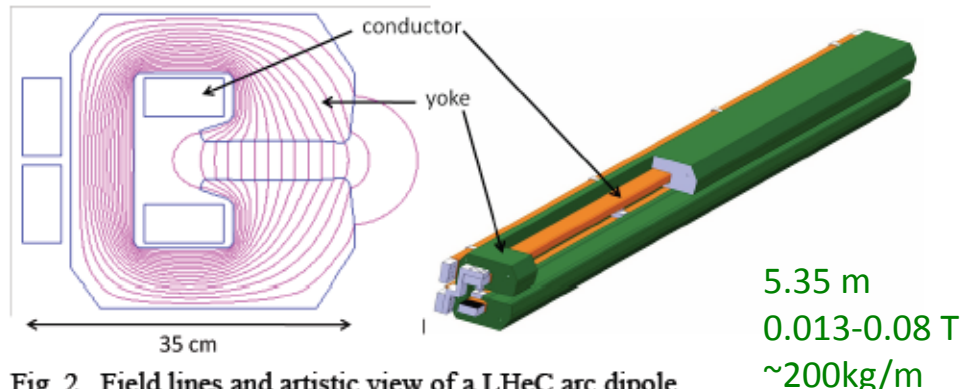


Fig. 2. Field lines and artistic view of a LHeC arc dipole.

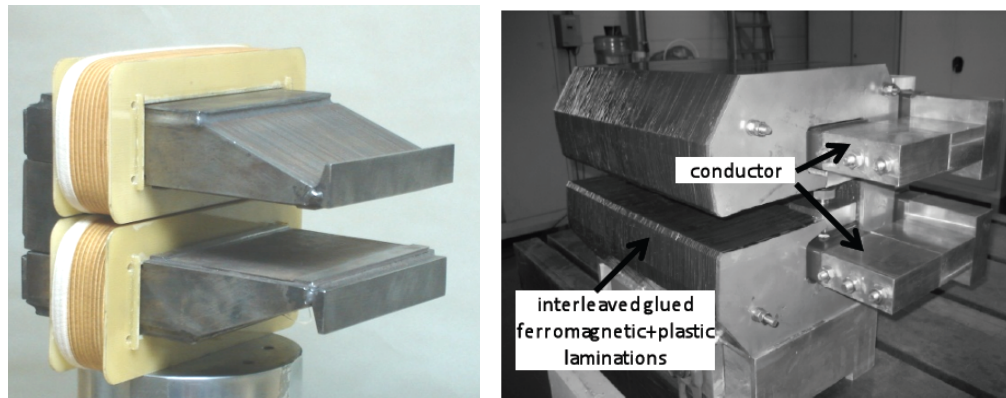
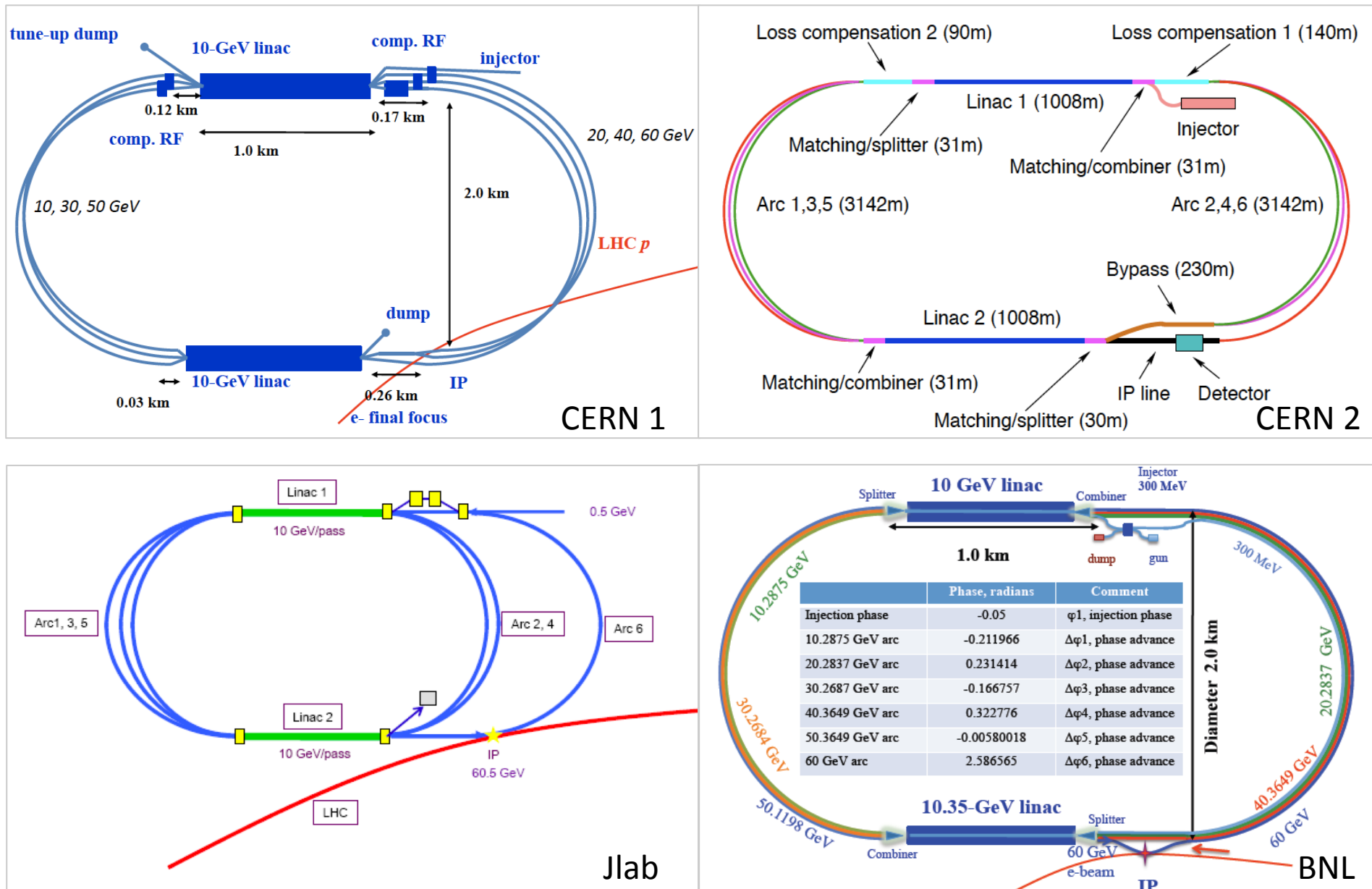


TABLE II REPRODUCIBILITY OF MAGNETIC FIELD OVER 8 CYCLES

Model	Low field	High fields
Maximum Relative Deviation from Average		
Model 1 (NiFe steel)	$5 \cdot 10^{-5}$	$4 \cdot 10^{-5}$
Model 2 (Low carbon steel)	$6 \cdot 10^{-5}$	$6 \cdot 10^{-5}$
Model 3 (Grain oriented 3.5% Si steel)	$4 \cdot 10^{-5}$	$6 \cdot 10^{-5}$
Standard Deviation from Average		
Model 1 (NiFe steel)	$3 \cdot 10^{-5}$	$3 \cdot 10^{-5}$
Model 2 (Low carbon steel)	$4 \cdot 10^{-5}$	$5 \cdot 10^{-5}$
Model 3 (Grain oriented 3.5% Si steel)	$2 \cdot 10^{-5}$	$4 \cdot 10^{-5}$

Prototypes from BINP and CERN: function to spec's

60 GeV Energy Recovery Linac



Two 10 GeV energy recovery Linacs, 3 returns, 720 MHz cavities

Linac Infrastructure

10 Civil Engineering and Services

- 10.1 Overview
- 10.2 Location, Geology and Construction Methods

 - 10.2.1 Location
 - 10.2.2 Land Features
 - 10.2.3 Geology
 - 10.2.4 Site Development
 - 10.2.5 Construction Methods

- 10.3 Civil Engineering Layouts for Ring-Ring
- 10.4 Civil Engineering Layouts for Linac-Ring
- 10.5 Summary

944 cavities
 59 cryo modules per linac
 721 MHz
 20 MV/m CW

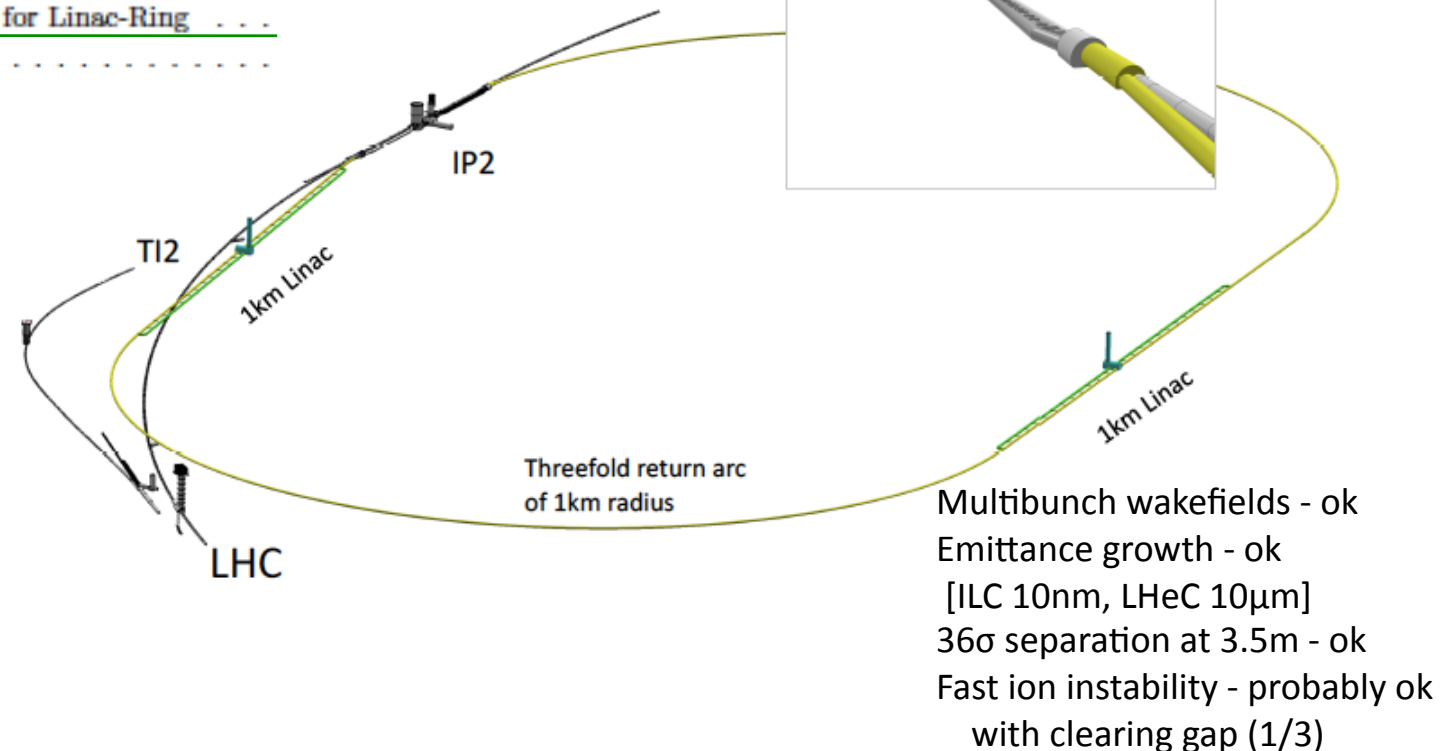


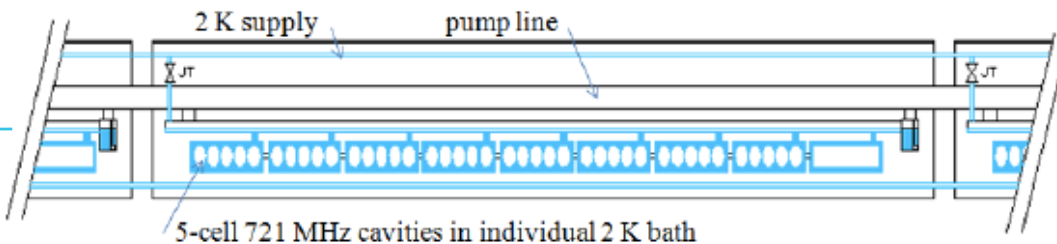
Figure 10.11: View on the ERL placed inside the LHC ring and tangential to IP2. TI2 is the injection line into the LHC. The insert shows the view towards IP2, which currently houses the ALICE experiment, from the direction of the protons colliding with the electron beam incoming from behind.

Cryogenics

9	System Design
9.1	Magnets for the Interaction Region
9.1.1	Introduction
9.1.2	Magnets for the ring-ring option
9.1.3	Magnets for the linac-ring option
9.2	Accelerator Magnets
9.2.1	Dipole Magnets
9.2.2	BINP Model
9.2.3	CERN Model
9.2.4	Quadrupole and Corrector Magnets
9.3	Ring-Ring RF Design
9.3.1	Design Parameters
9.3.2	Cavities and klystrons
9.4	Linac-Ring RF Design
9.4.1	Design Parameters
9.4.2	Layout and RF powering
9.4.3	Arc RF systems
9.5	Crab crossing for the LHeC
9.5.1	Luminosity Reduction
9.5.2	Crossing Schemes
9.5.3	RF Technology
9.6	Vacuum
9.6.1	Vacuum requirements
9.6.2	Synchrotron radiation
9.6.3	Vacuum engineering issues
9.7	Beam Pipe Design
9.7.1	Requirements
9.7.2	Choice of Materials for beampipes
9.7.3	Beampipe Geometries
9.7.4	Vacuum Instrumentation
9.7.5	Synchrotron Radiation Masks
9.7.6	Installation and Integration
9.8	Cryogenics
9.8.1	Ring-Ring Cryogenics Design
9.8.2	Linac-Ring Cryogenics Design
9.8.3	General Conclusions Cryogenics for LHeC
9.9	Beam Dumps and Injection Regions
9.9.1	Injection Region Design for Ring-Ring Option
9.9.2	Injection transfer line for the Ring-Ring Option
9.9.3	60 GeV internal dump for Ring-Ring Option
9.9.4	Post collision line for 140 GeV Linac-Ring option
9.9.5	Absorber for 140 GeV Linac-Ring option
9.9.6	Energy deposition studies for the Linac-Ring option
9.9.7	Beam line dump for ERL Linac-Ring option
9.9.8	Absorber for ERL Linac-Ring option

Table 2: Components of the Electron Accelerators

	Ring	Linac
magnets		
beam energy		60 GeV
number of dipoles	3080	3600
dipole field [T]	0.013 – 0.076	0.046 – 0.264
total nr of quads	866	1588
RF and cryogenics		
number of cavities	112	944
gradient [MV/m]	11.9	20
RF power [MW]	49	39
cavity voltage [MV]	5	21.2
cavity $R/Q [\Omega]$	114	285
cavity Q_0	—	$2.5 \cdot 10^{10}$
cooling power [kW]	5.4@4.2 K	30@2 K



systems will consist of a complex task. Further cavities and cryomodules will require a limited R&D program. From this we expect improved quality factors with respect to today's state of the art. The cryogenics of the L-R version consists of a formidable engineering challenge, however, it is feasible and, CERN disposes of the respective know-how.

IV Detector

12 Detector Requirements

12.1 Requirements on the LHeC Detector
12.1.1 Installation and Magnets
12.1.2 Kinematic reconstruction
12.1.3 Acceptance regions - scattered electron
12.1.4 Acceptance regions - hadronic final state
12.1.5 Acceptance at the High Energy LHC
12.1.6 Energy Resolution and Calibration
12.1.7 Tracking Requirements
12.1.8 Particle Identification Requirements
12.1.9 Summary of the Requirements on the LHeC Detector

13 Central Detector

13.1 Basic Detector Description
13.1.1 Baseline Detector Layout
13.1.2 An Alternative Solenoid Placement - Option B
13.2 Magnet Design
13.2.1 Magnets configuration
13.2.2 Detector Solenoid
13.2.3 Detector integrated e-beam bending dipoles
13.2.4 Cryogenics for magnets and calorimeter
13.2.5 Twin Solenoid System
13.3 Tracking Detector
13.3.1 Tracking Detector - Baseline Layout
13.3.2 Performance
13.3.3 Tracking detector design criteria and possible solutions
13.4 Calorimetry
13.4.1 The Barrel Electromagnetic Calorimeter
13.4.2 The Hadronic Barrel Calorimeter
13.4.3 Endcap Calorimeters
13.5 Calorimeter Simulation
13.5.1 The Barrel LAr Calorimeter Simulation
13.5.2 The Barrel Tile Calorimeter Simulation
13.5.3 Combined Liquid Argon and Tile Calorimeter Simulation
13.5.4 Lead-Scintillator Electromagnetic Option
13.5.5 Forward and Backward Inserts Calorimeter Simulation
13.6 Calorimeter Summary
13.7 Muon Detector
13.7.1 Muon detector design
13.7.2 The LHeC muon detector options
13.7.3 Forward Muon Extensions
13.7.4 Muon Detector Summary
13.8 Event and Detector Simulations
13.8.1 Pythia6
13.8.2 1 MeV Neutron Equivalent
13.8.3 Nearest Neighbor
13.8.4 Cross Checking
13.8.5 Future Goals

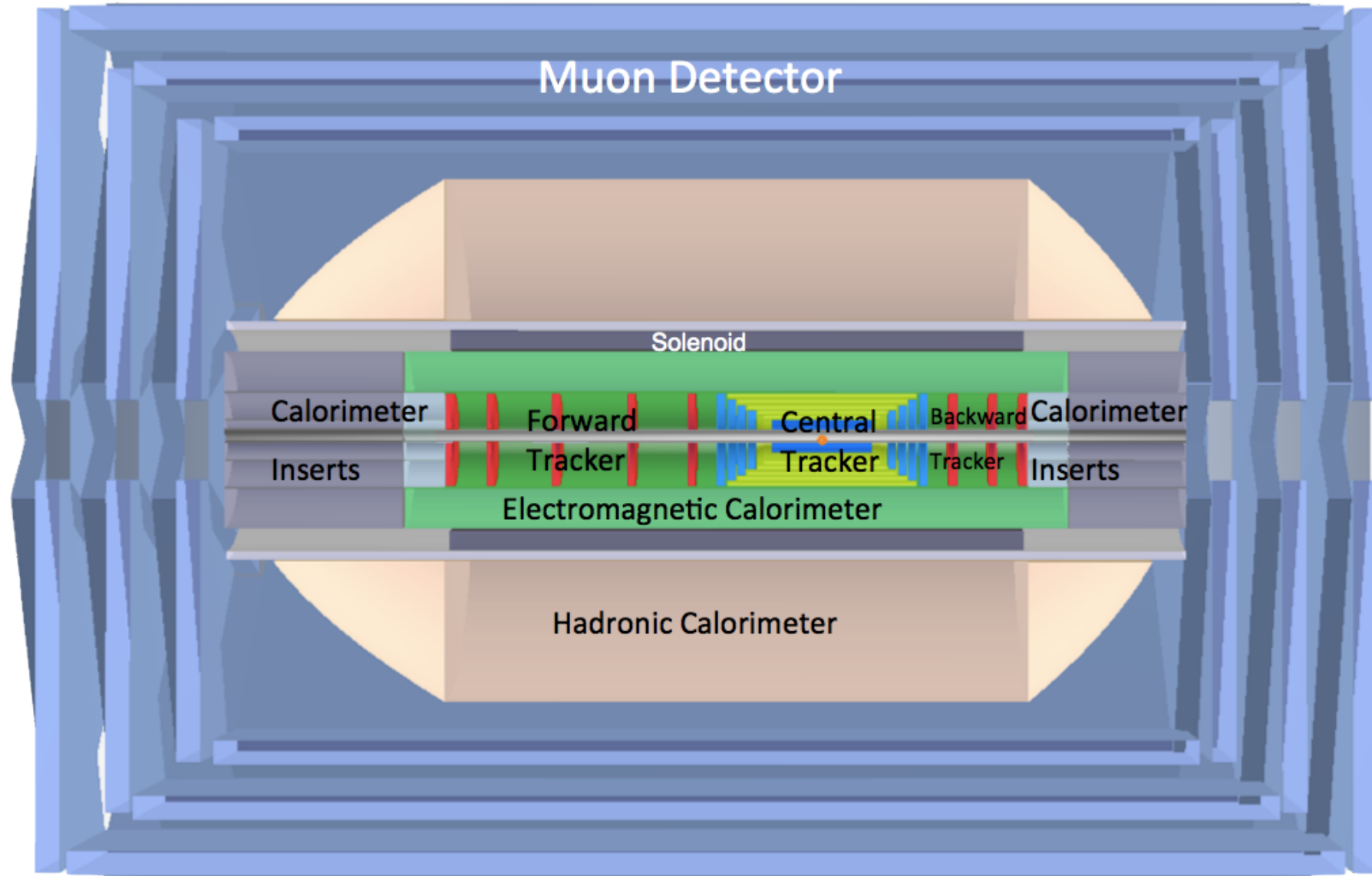
14 Forward and Backward Detectors

14.1 Luminosity Measurement and Electron Tagging
14.1.1 Options
14.1.2 Use of the Main LHeC Detector
14.1.3 Dedicated Luminosity Detectors in the tunnel
14.1.4 Small angle Electron Tagger
14.1.5 Summary and Open Questions
14.2 Polarimeter
14.2.1 Polarisation from the scattered photons
14.2.2 Polarisation from the scattered electrons
14.3 Zero Degree Calorimeter
14.3.1 ZDC detector design
14.3.2 Neutron Calorimeter
14.3.3 Proton Calorimeter
14.3.4 Calibration and monitoring
14.4 Forward Proton Detection

Detector Requirements

-
- The diagram illustrates the LHeC detector's layout. It features a central vertical solenoid surrounded by two sets of dipole magnets, one on each side. The central region is labeled 'Solenoid'. The outer regions are labeled 'Dipoles'. Below the solenoid, there are several horizontal layers representing different detector components: 'Inserts' (red), 'Electromagnetic Calorimeter' (green), 'Hadronic Calorimeter' (blue), 'Tracker' (yellow), and 'Inserts' (red). Arrows point from the text descriptions to specific parts of the detector diagram.
- **High Precision**
resolution, calibration, low noise at low y , tagging of b,c;
 - Based on the recent detector developments, “settled” technology,
avoiding time consuming dedicated R&D programs.
 - Modular for installation and flexible for access
Detector construction above ground (LHC schedule!)
 - Small radius and thickness of beam pipe optimized in view of
1-179° acceptance [for low x, Q^2 (e) as for high x (final state)],
synchrotron radiation and background production.
 - Affordable - comparatively reasonable cost.
 - One IR, one detector (no push-pull, two teams/reconstructions..?)

LHeC Detector Overview



Detector option 1 for LR and full acceptance coverage

Forward/backward asymmetry in energy deposited and thus in geometry and technology

Present dimensions: $L \times D = 14 \times 9 \text{ m}^2$ [CMS $21 \times 15 \text{ m}^2$, ATLAS $45 \times 25 \text{ m}^2$]

Taggers at -62m (e), 100m (γ ,LR), -22.4m (γ ,RR), +100m (n), +420m (p)

Detector Magnets

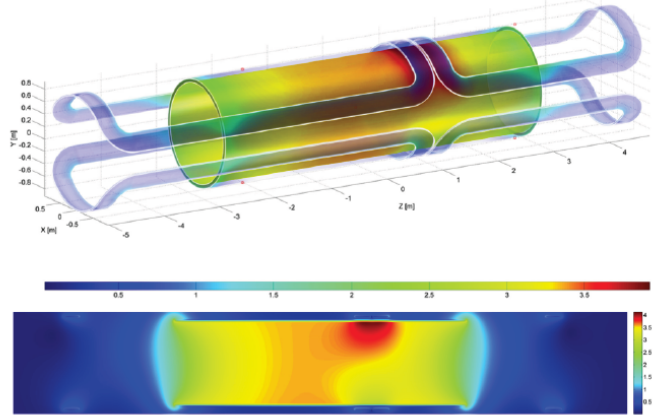


Figure 13.13: Magnetic field of the magnet system of solenoid and the two internal superconducting dipoles at nominal currents (effect of iron ignored). The position of the peak magnetic field of 3.9 T is local due to the adjacent current return heads on top of the solenoid where all magnetic fields add up.

Dipole (for head on LR) and
solenoid in common cryostat,
perhaps with electromagnetic LAr

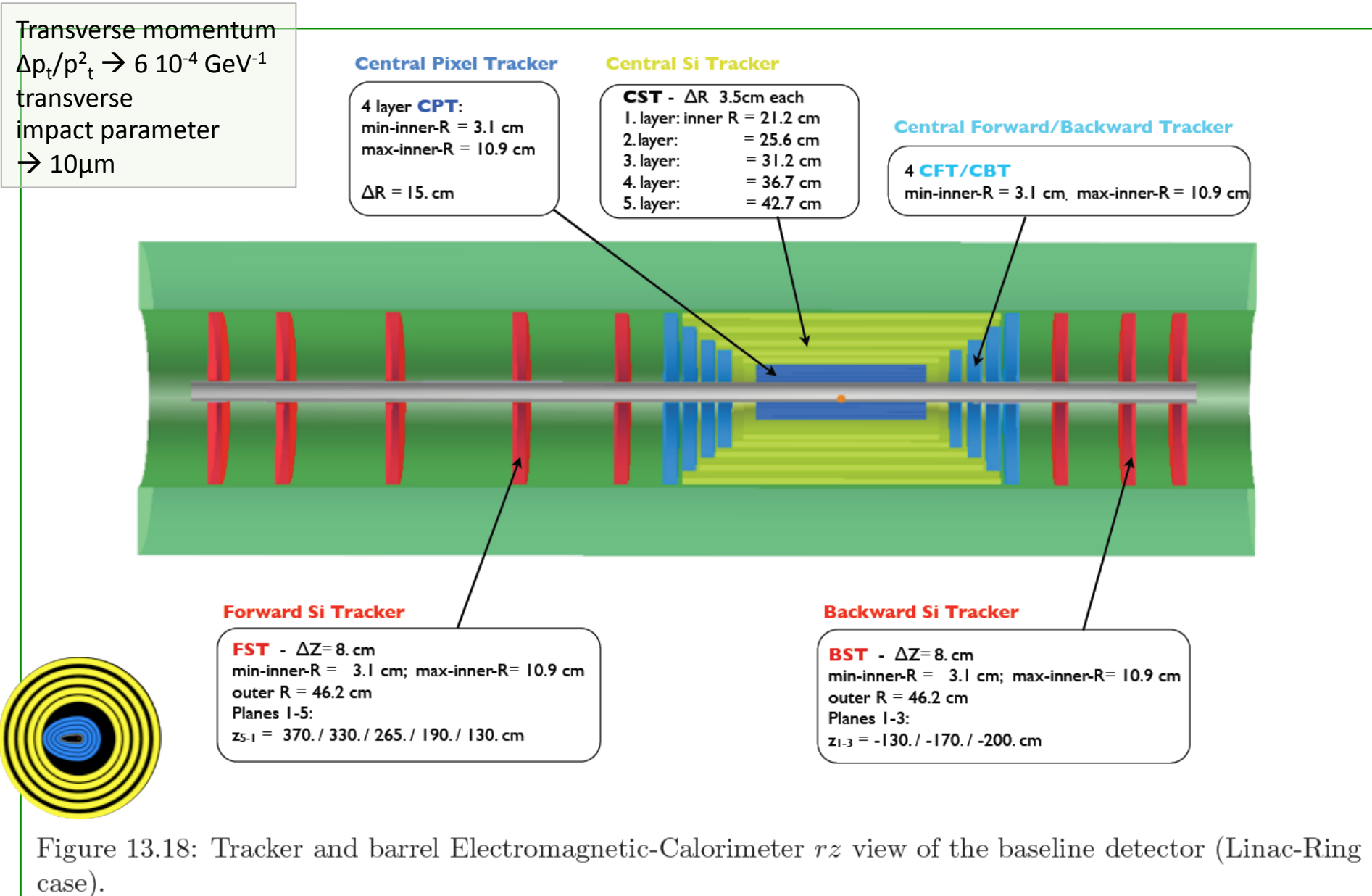
3.5T field at ~1m radius to house
a Silicon tracker

Based on ATLAS+CMS experience

Property	Parameter	value	unit
Dimensions	Cryostat inner radius	0.900	m
	Length	10.000	m
	Outer radius	1.140	m
	Coil windings inner radius	0.960	m
	Length	5.700	m
	Thickness	60.0	mm
	Support cylinder thickness	0.030	m
	Conductor section, Al-stabilized NbTi/Cu + insulation	30.0×6.8	mm^2
	Length	10.8	km
	Superconducting cable section, 20 strands	12.4×2.4	mm^2
Masses	Superconducting strand diameter Cu/NbTi ratio = 1.25	1.24	mm
	Conductor windings	5.7	t
	Support cylinder, solenoid section + dipole sections	5.6	t
	Total cold mass	12.8	t
	Cryostat including thermal shield	11.2	t
Electro-magnetics	Total mass of cryostat, solenoid and small parts	24	t
	Central magnetic field	3.50	T
	Peak magnetic field in windings (dipoles off)	3.53	T
	Peak magnetic field in solenoid windings (dipoles on)	3.9	T
	Nominal current	10.0	kA
	Number of turns, 2 layers	1683	
	Self-inductance	1.7	H
	Stored energy	82	MJ
	E/m, energy-to-mass ratio of windings	14.2	kJ/kg
	E/m, energy-to-mass ratio of cold mass	9.2	kJ/kg
Margins	Charging time	1.0	hour
	Current rate	2.8	A/s
	Inductive charging voltage	2.3	V
	Coil operating point, nominal / critical current	0.3	
Mechanics	Temperature margin at 4.6 K operating temperature	2.0	K
	Cold mass temperature at quench (no extraction)	~ 80	K
	Mean hoop stress	~ 55	MPa
Cryogenics	Peak stress	~ 85	MPa
	Thermal load at 4.6 K, coil with 50% margin	~ 110	W
	Radiation shield load width 50% margin	~ 650	W
	Cooling down time / quench recovery time	4 and 1	day
	Use of liquid helium	~ 1.5	g/s

Table 13.1: Main parameters of the baseline LHeC Solenoid providing 3.5 T in a free bore of 1.8 m.

Silicon Tracker and EM Calorimeter



Liquid Argon Electromagnetic Calorimeter

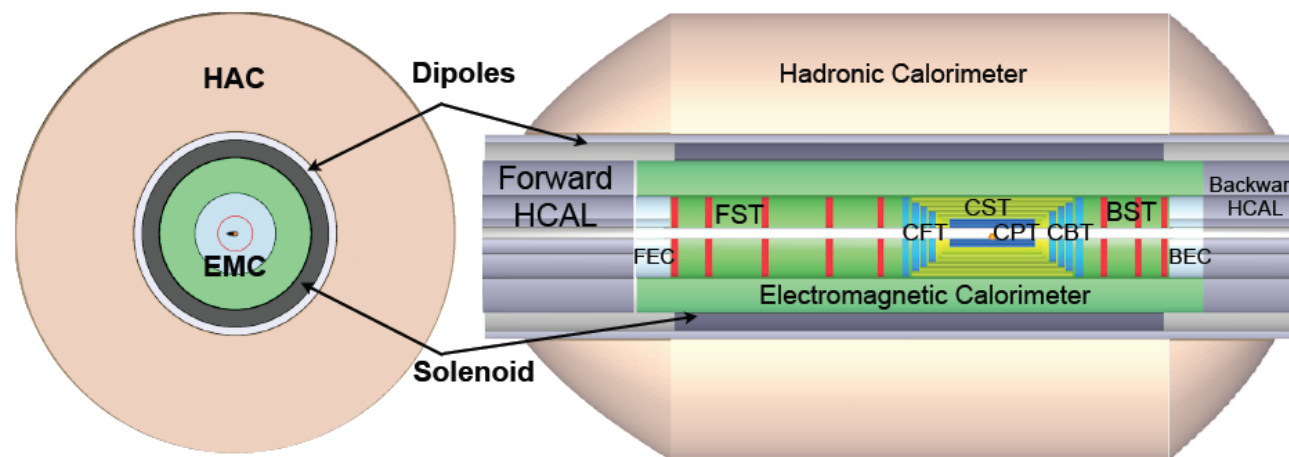


Figure 13.30: x - y and r - z view of the LHeC Barrel EM calorimeter (green).

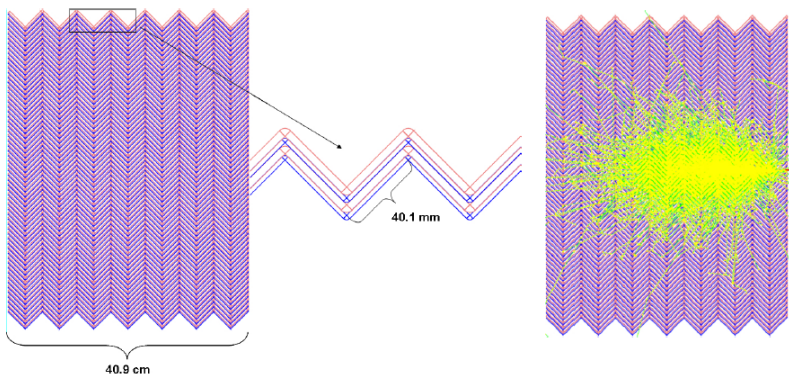


Figure 13.35: View of the parallel geometry accordion calorimeter (left) and simulation of a single electron shower with initial energy of 20 GeV (right).

GEANT4 Simulation

Inside Coil
H1, ATLAS
experience.

Barrel: Pb, $20 X_0$, 11m^3

fwd/bwd inserts:

FEC: Si -W, $30 X_0$, 0.3m^3

BEC: Si -Pb, $25 X_0$, 0.3m^3

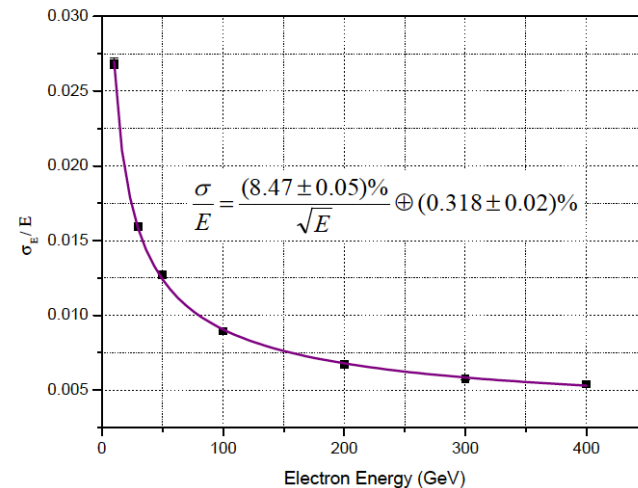


Figure 13.36: LAr accordion calorimeter energy resolution for electrons between 10 and 400 GeV.

Hadronic Tile Calorimeter

E-Cal Parts	FEC1	FEC2		EMC		BEC2	BEC1
Min. Inner radius R [cm]	3.1	21		48		21	3.1
Min. polar angle θ [$^{\circ}$]	0.48	3.2		6.6/168.9		174.2	179.1
Max. pseudorapidity η	5.5	3.6		2.8/-2.3		-3.	-4.8
Outer radius [cm]	20	46		88		46	20
z -length [cm]	40	40		660		40	40
Volume [m^3]				11.3			0.3

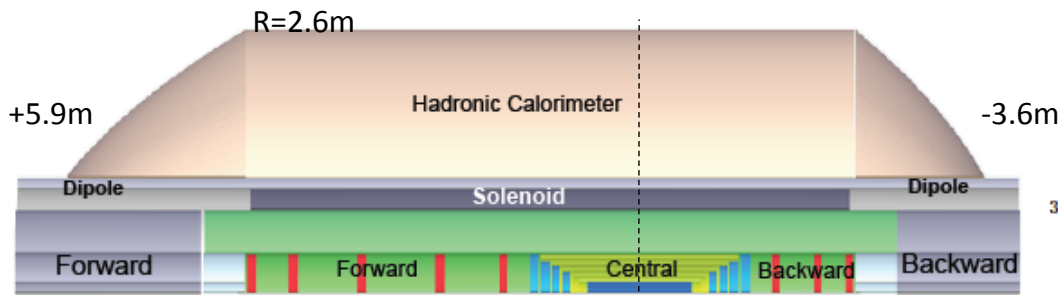
H-Cal Parts barrel			FHC4	HAC	BHC4		
Inner radius [cm]			120	120	120		
Outer radius [cm]			260	260	260		
z -length [cm]			217	580	157		
Volume [m^3]				121.2			

H-Cal Parts Inserts	FHC1	FHC2	FHC3		BHC3	BHC2	BHC1
Min. inner radius R [cm]	11	21	48		48	21	11
Min. polar angle θ [$^{\circ}$]	0.43	2.9	6.6		169.	175.2	179.3
Max/min pseudorapidity η	5.6	3.7	2.9		-2.4	-3.2	-5.
Outer radius [cm]	20	46	88		88	46	20
z -length [cm]	177	177	177		117	117	117
Volume [m^3]			4.2			2.8	

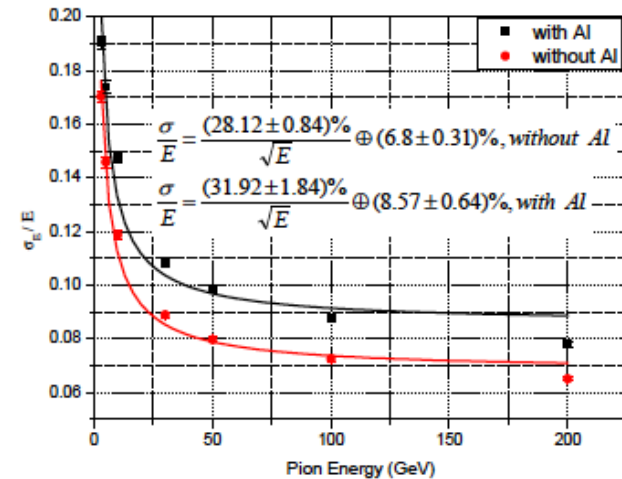
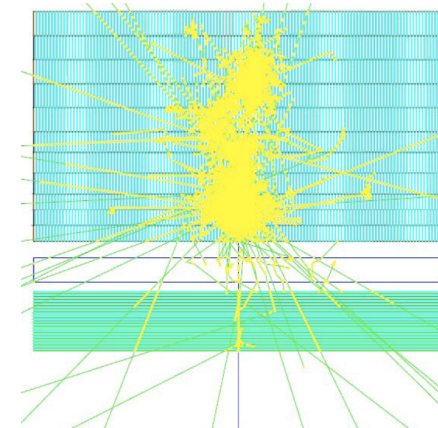
Table 13.6: Summary of calorimeter dimensions.

The electromagnetic barrel calorimeter is currently represented by the barrel part EMC (LAr-Pb module); the setup reaches $X_0 \approx 25$ radiation length) and the movable inserts forward FEC1, FEC2 (Si-W modules ($X_0 \approx 30$) and the backward BEC1, BEC2 (Si-Pb modules; $X_0 \approx 25$).

The hadronic barrel parts are represented by FHC4, HAC, BHC4 (forward, central and backward - Scintillator-Fe Tile modules; $\lambda_I \approx 8$ interaction length) and the movable inserts FHC1, FHC2, FHC3 (Si-W modules; $\lambda_I \approx 10$), BHC1, BHC2, BHC3 (Si-Cu modules, $\lambda_I \approx 8$) see Fig. 13.9.



Outside Coil: flux return
Modular. ATLAS experience.

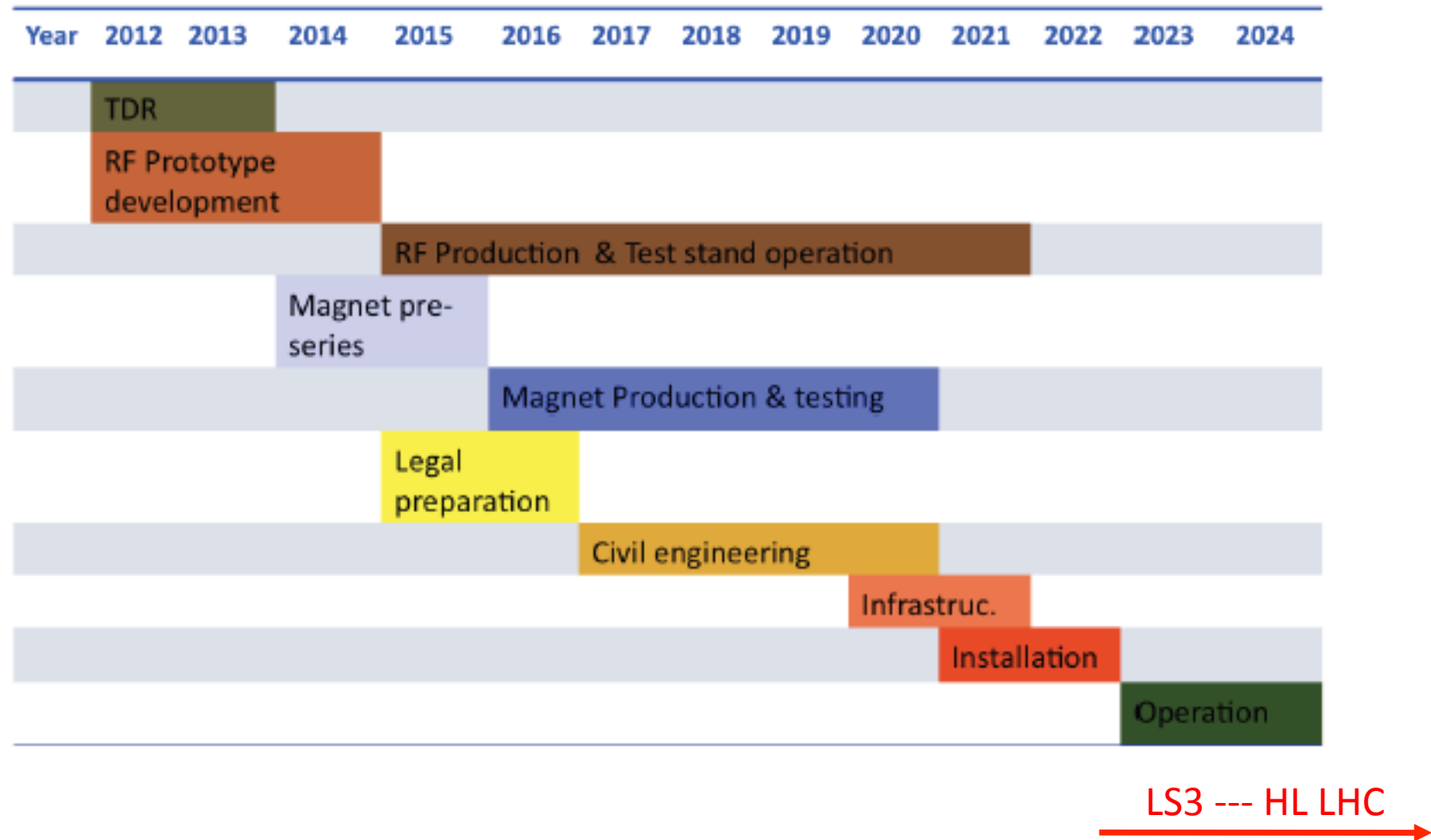


3.37: Accordion and Tile Calorimeter energy resolution for pions with and without 14cm Al block.

Combined GEANT4 Calorimeter Simulation

Outlook

Tentative Time Schedule



We base our estimates for the project time line on the experience of other projects, such as (LEP, LHC and LINAC4 at CERN and the European XFEL at DESY and the PSI XFEL)

from draft CDR

Draft LHC Schedule for the coming decade

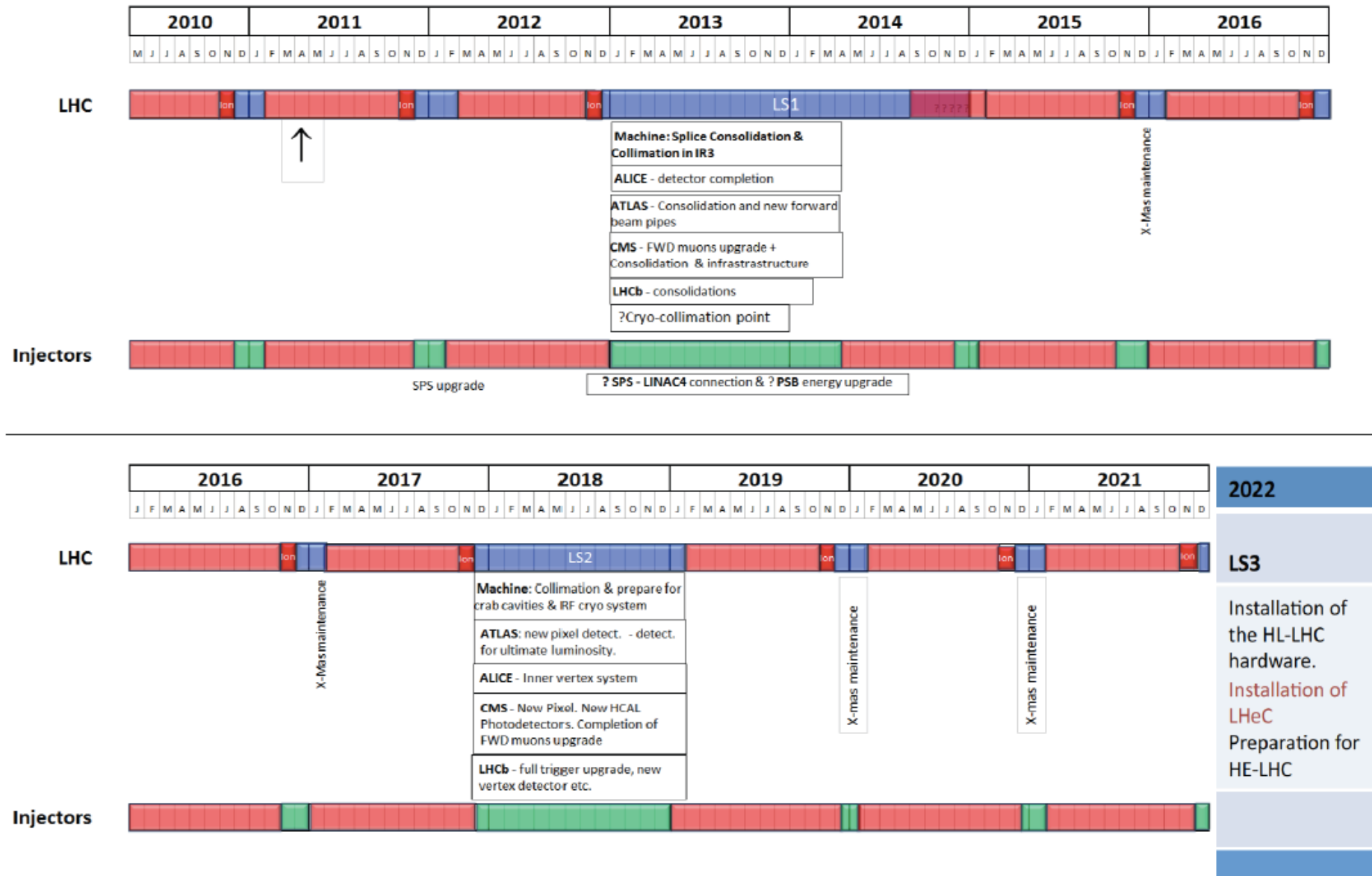


Figure 11.1: CERN medium term plan (MTP), draft as of July 2011
as shown by S. Myers at EPS 2011 Grenoble

Summary

Table 1: Parameters of the RR and RL Configurations

	Ring	Linac
electron beam		
beam energy E_e		60 GeV
$e^- (e^+)$ per bunch $N_e [10^9]$	20 (20)	1 (0.1)
$e^- (e^+)$ polarisation [%]	40 (40)	90 (0)
bunch length [mm]	10	0.6
tr. emittance at IP $\gamma \epsilon_{x,y}^e$ [mm]	0.58, 0.29	0.05
IP β function $\beta_{x,y}^*$ [m]	0.4, 0.2	0.12
beam current [mA]	131	6.6
energy recovery intensity gain	—	17
total wall plug power		100 MW
syn rad power [kW]	51	49
critical energy [keV]	163	718
proton beam		
beam energy E_p		7 TeV
protons per bunch N_p		$1.7 \cdot 10^{11}$
transverse emittance $\gamma \epsilon_{x,y}^p$		3.75 μm
collider		
Lum $e^- p (e^+ p) [10^{32}\text{cm}^{-2}\text{s}^{-1}]$	9 (9)	10 (1)
bunch spacing		25 ns
rms beam spot size $\sigma_{x,y}$ [μm]	30, 16	7
crossing angle θ [mrad]	1	0
$L_{eN} = A L_{eA} [10^{32}\text{cm}^{-2}\text{s}^{-1}]$	0.3	1

Both the ring and the linac are feasible and both come very close to the desired performance.
The pleasant challenge is to soon decide for one.

CERN-ECFA-NuPECC:

CDR Draft (530pages) being refereed
Publish spring 2012

Steps towards TDR (tentative)

- Prototype IR magnet (3 beams)
- Prototype Dipole (1:1)
- Develop Cavity/Cryomodule
- Civil Engineering, ...

Build international collaborations

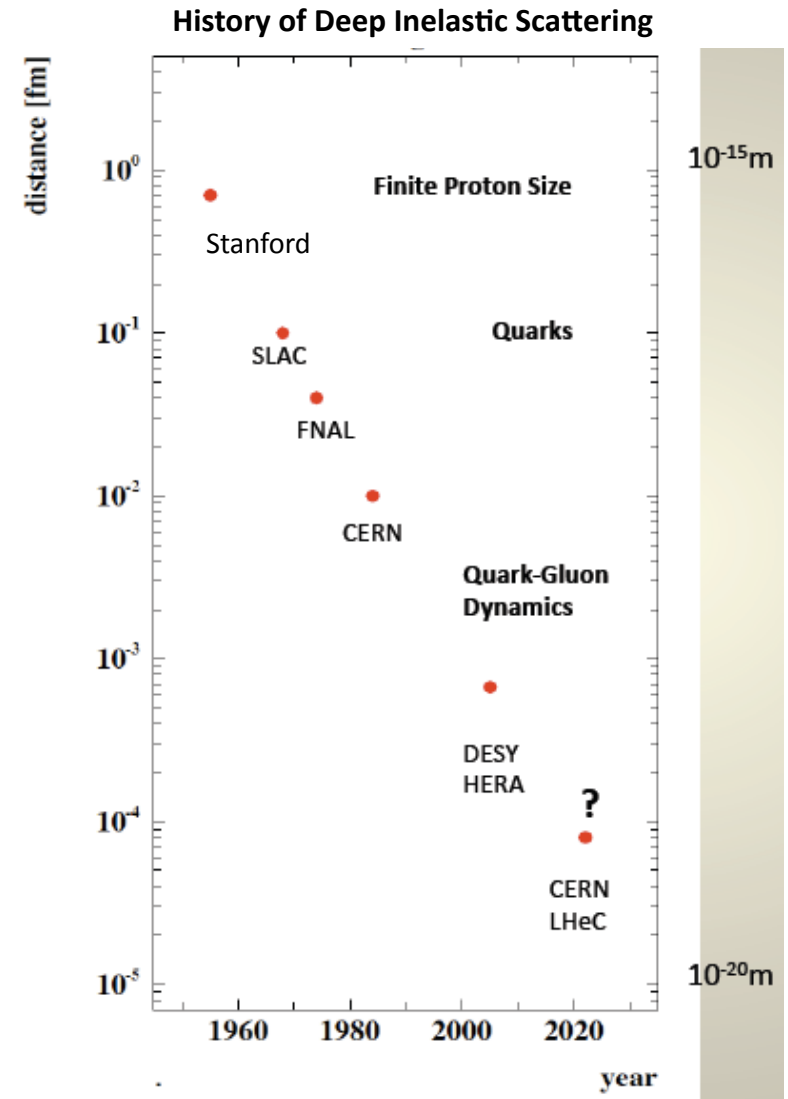
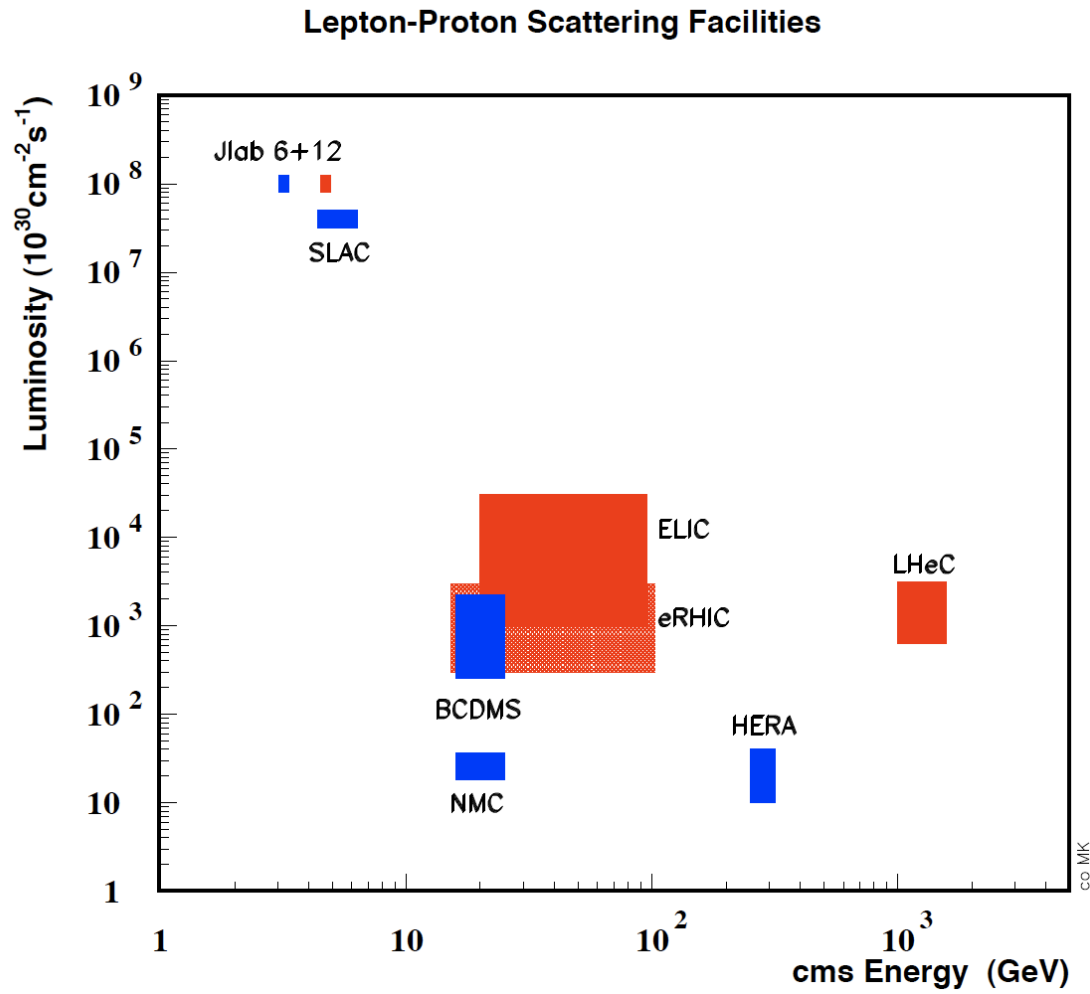
for the accelerator and detector development. Strong links to ongoing accelerator and detector projects.

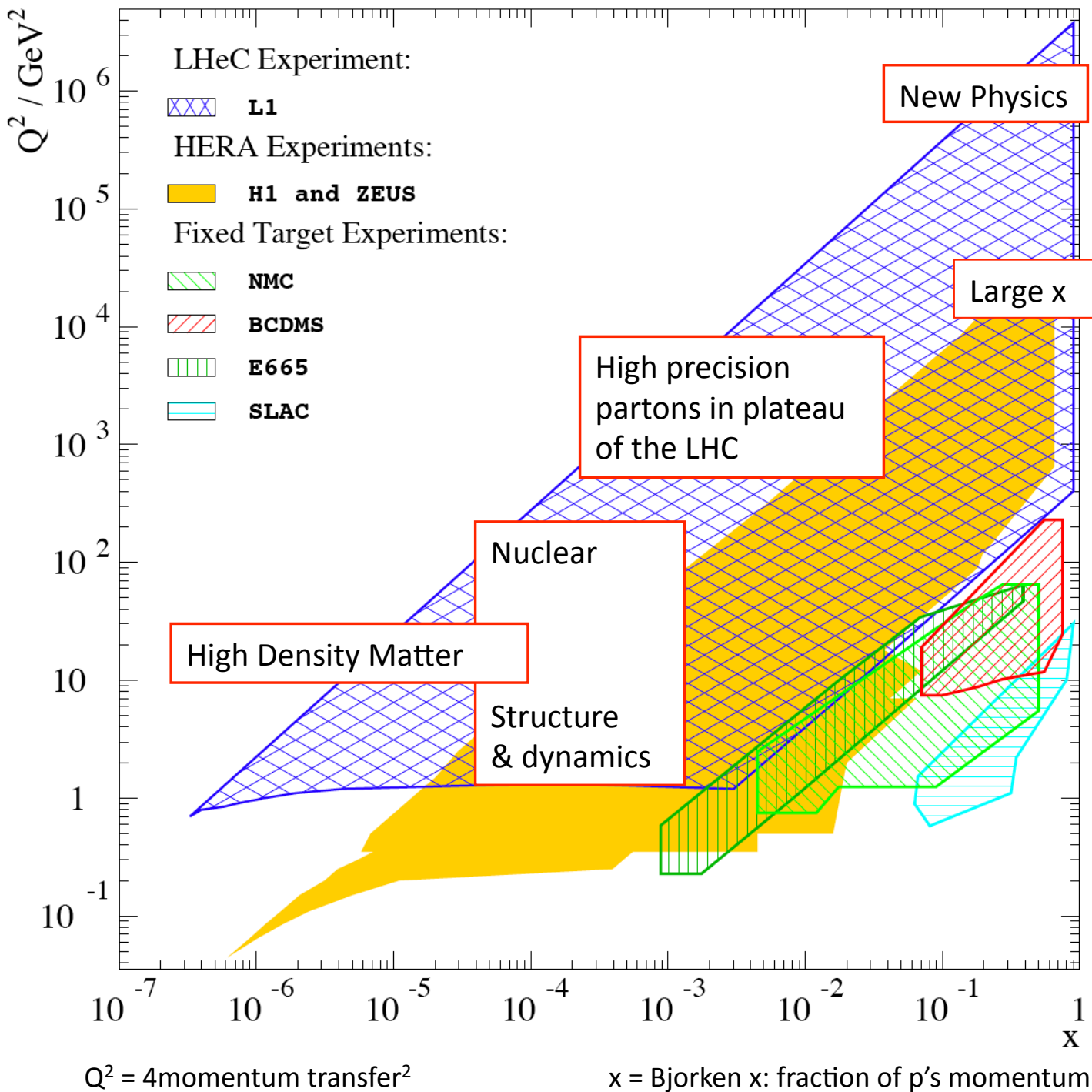
The LHC offers the unique perspective for a further TeV scale collider. The LINAC's are of about 2 mile length, yet the Q^2 is 10^5 times larger than was achieved when SLAC discovered quarks. Particle physics needs pp, ll and ep.

Here is a realistic prospect to progress
You are cordially invited to join

backup

Deep Inelastic Scattering - History and Prospects





Why an ep/A Experiment at TeV Energies?

1. For resolving the quark structure of the nucleon with p, d and ion beams
QPM symmetries, quark distributions (complete set from data!), GPDs, nuclear PDFs ..
2. For the development of perturbative QCD [37-28-15]
 $N^k LO$ ($k \geq 2$) and h.o. eweak, HQs, jets, resummation, factorisation, diffraction
3. For mapping the gluon field
Gluon for $\sim 10^{-5} < x < 1$, is unitarity violated? J/ψ , F_2^c , ... unintegrated gluon
4. For searches and the understanding of new physics
GUT (α_s to 0.1%), LQs RPV, Higgs (bb, HWW) ... PDFs4LHC... instanton, odderon,..?
5. For investigating the physics of parton saturation
Non-pQCD (chiral symm breaking, confinement), black disc limit, saturation border..

..For providing data which could be of use for future experiments [Proposal for SLAC ep 1968]

Summary of Design Parameters

electron beam	RR	LR	LR
e- energy at IP[GeV]	60	60	140
luminosity [$10^{32} \text{ cm}^{-2}\text{s}^{-1}$]	17	10	0.44
polarization [%]	40	90	90
bunch population [10^9]	26	2.0	1.6
e- bunch length [mm]	10	0.3	0.3
bunch interval [ns]	25	50	50
transv. emit. $\gamma\varepsilon_{x,y}$ [mm]	0.58, 0.29	0.05	0.1
rms IP beam size $\sigma_{x,y}$ [μm]	30, 16	7	7
e- IP beta funct. $\beta_{x,y}^*$ [m]	0.18, 0.10	0.12	0.14
full crossing angle [mrad]	0.93	0	0
geometric reduction H_{hg}	0.77	0.91	0.94
repetition rate [Hz]	N/A	N/A	10
beam pulse length [ms]	N/A	N/A	5
ER efficiency	N/A	94%	N/A
average current [mA]	131	6.6	5.4
tot. wall plug power[MW]	100	100	100

High E_e Linac option (ERL?) if physics demands HE-LHC?

proton beam	RR	LR
bunch pop. [10^{11}]	1.7	1.7
tr.emit. $\gamma\varepsilon_{x,y}$ [μm]	3.75	3.75
spot size $\sigma_{x,y}$ [μm]	30, 16	7
$\beta_{x,y}^*$ [m]	1.8, 0.5	0.1
bunch spacing [ns]	25	25

“ultimate p beam”
1.7 probably conservative
and emittance too

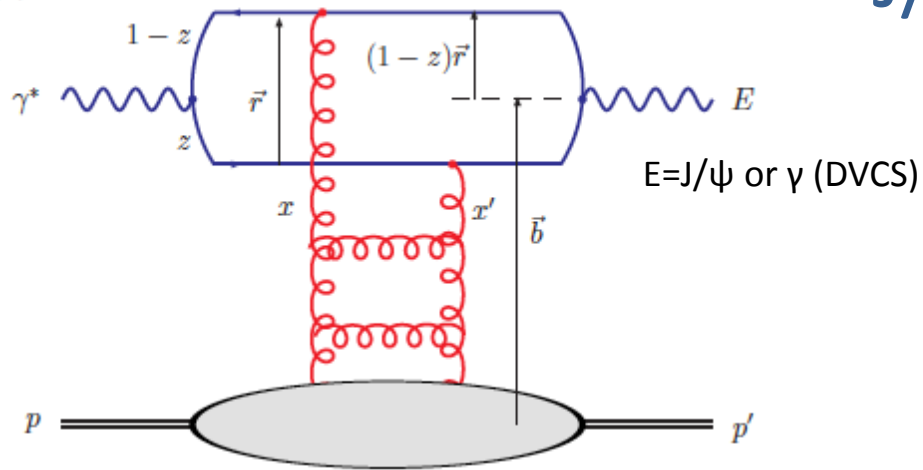
CDR has design also for
D and A ($L_{eN} \approx 3 * 10^{31} \text{ cm}^{-2}\text{s}^{-1}$)

RR= Ring – Ring
LR =Linac –Ring

Ring: use 1° as baseline : L/2
Linac: clearing gap: L*2/3

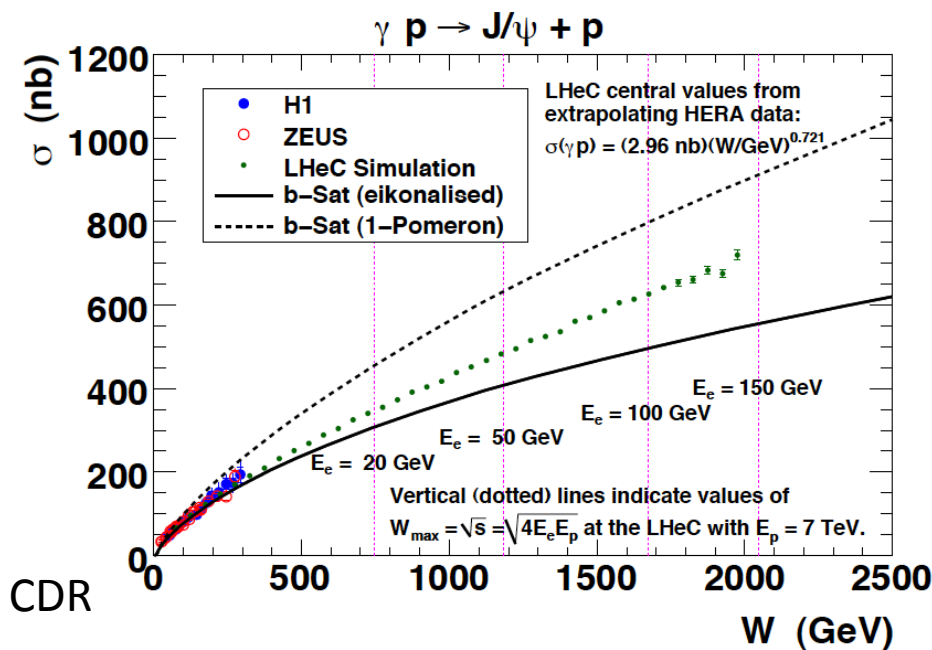
J/ ψ in $\gamma^* p/A$

(a)

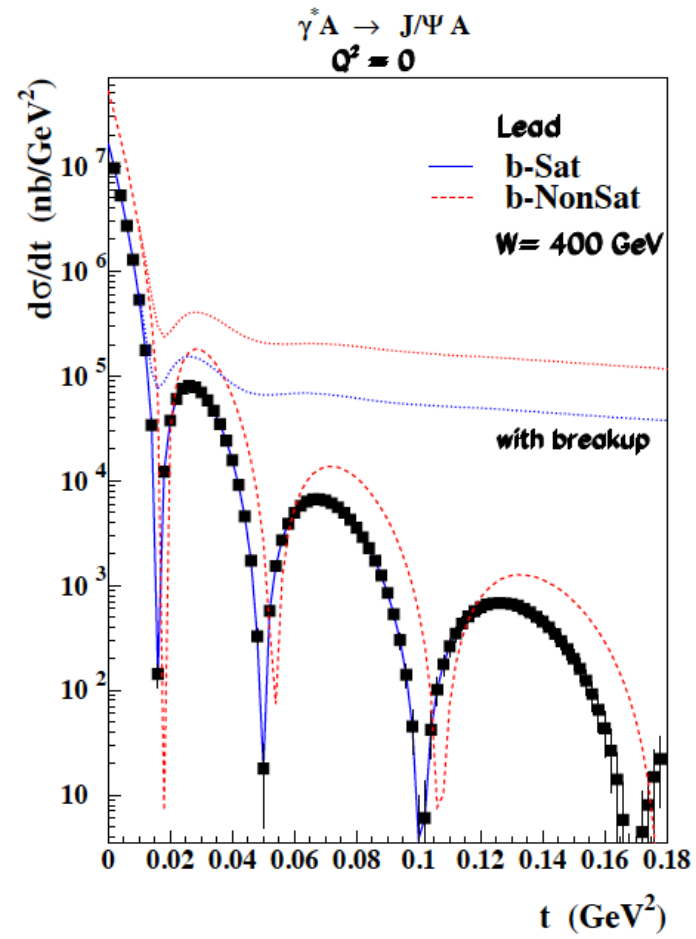


$$\sigma_{T,L}^{\gamma^* p}(x, Q) = \text{Im } \mathcal{A}_{T,L}^{\gamma^* p \rightarrow \gamma^* p}(x, Q, \Delta = 0) = \sum_f \int d^2r \int_0^1 dz \frac{1}{4\pi} (\Psi^* \Psi)_T^f \int d^2b \frac{d\sigma_{qq}}{d^2b}$$

Optical theorem relates J/ψ to $F_T = F_2 - F_L$



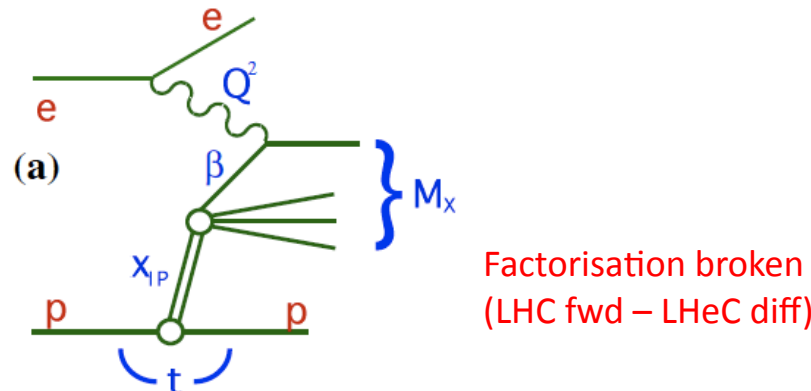
Test of saturation



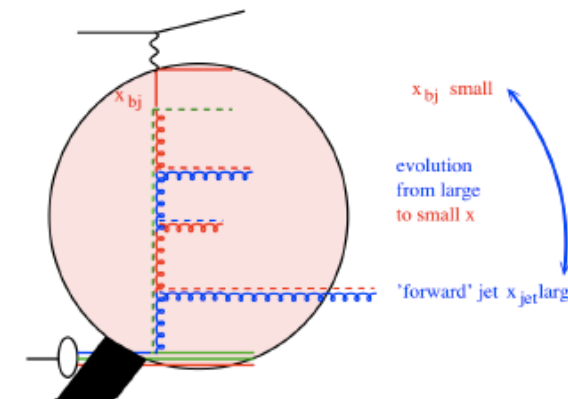
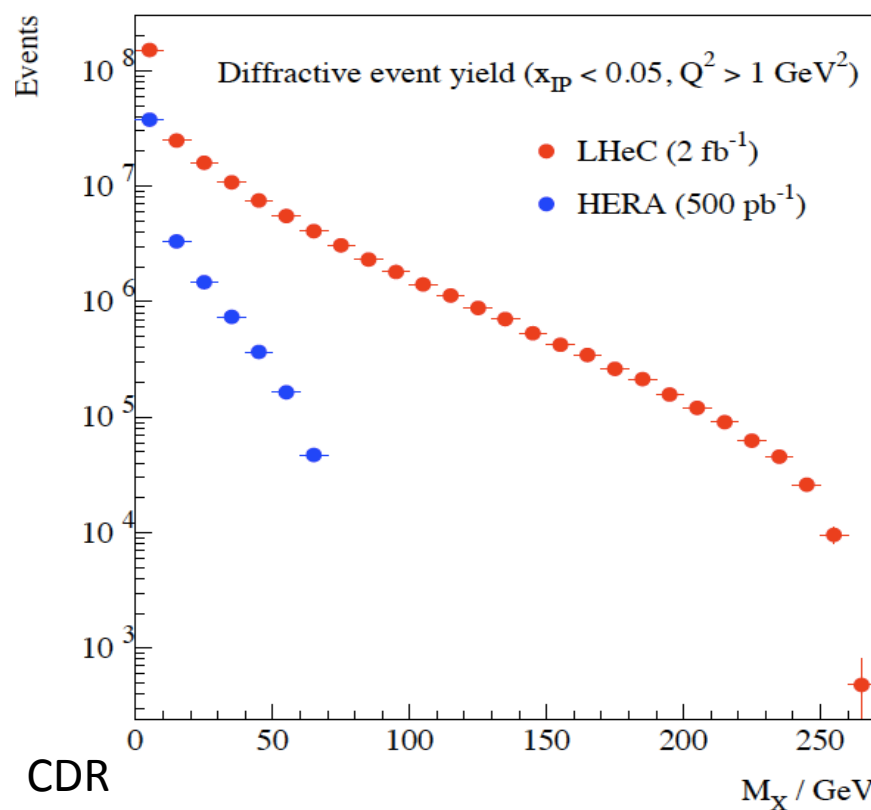
Coherent production in $\gamma^* A$

Probing of nuclear matter

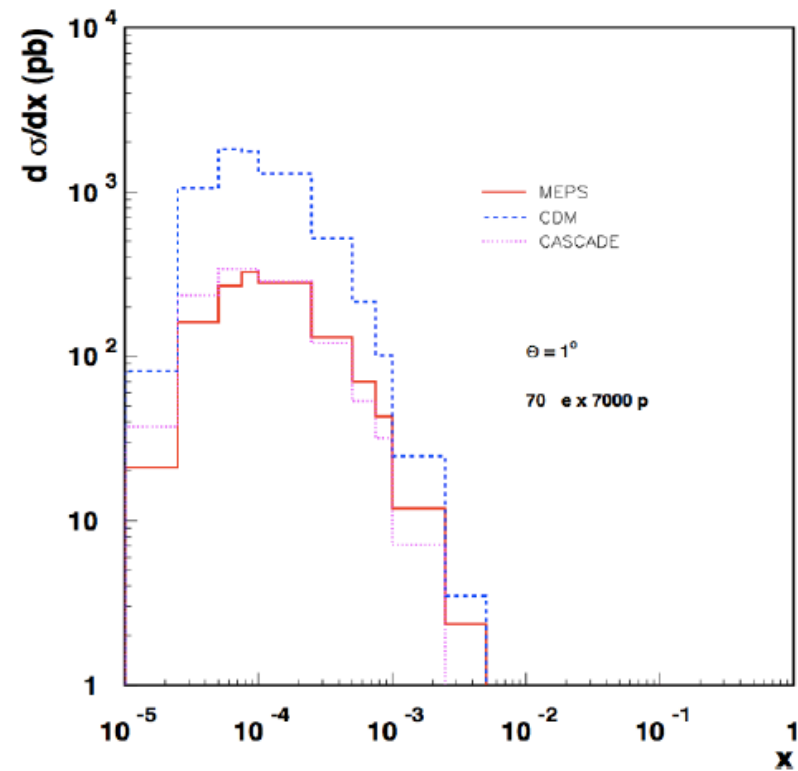
Quark-Gluon Dynamics - Diffraction and HFS (fwd jets)



Production of high mass 1^- states



Understand multi-jet emission (uninteg. pdf's), tune MC's



At HERA resolved γ effects mimic non-kt ordered emission